Development and validation of transgene constructs in order to generate bi-transgenic mice models for Diabetic Peripheral Neuropathy research

By

Lakshmy Nair

Submitted to the graduate degree program in Pharmacology and Toxicology and the Graduate Faculty of the University of Kansas in partial fulfillment of the requirements for the degree of Master's of Science.

_____

Dr. Rick Thomas Dobrowsky, Professor and Chairperson of the Thesis Committee

_____

Dr. Jeffrey Leonard Staudinger, Associate Professor and Committee Member

_____

Dr. David Davido, Assistant Professor and Committee Member

Date submitted: _____

The Thesis Committee for Lakshmy Nair certifies that this is the approved Version of the following thesis:

Development and validation of transgene constructs in order to generate bi-transgenic mice models for Diabetic Peripheral Neuropathy research

Committee:

_____
Dr. Rick Thomas Dobrowsky, Professor and Chairperson of the Thesis Committee

_____
Dr. Jeffrey Leonard Staudinger, Associate Professor and Committee Member

_____
Dr. David Davido, Assistant Professor and Committee Member

Date approved: _____

ABSTRACT

Diabetic peripheral neuropathy (DPN), a common complication of diabetes, involves nerve damage in the arms and legs. Segmental demyelination is one of the basic patterns observed in the pathology of DPN. Demyelinating neuropathies are those in which the Schwann cells (SCs) are primarily affected and these undergo substantial degeneration in diabetic neuropathy. Hence, it is of pertinence to investigate possible mechanisms which may contribute to the demyelination of SCs and the progression of DPN. To address this issue, this project aims to generate three different bi-transgenic mouse models that provide for the SC-specific expression of several transgenes that can be induced by the addition of the antibiotic doxycycline.

For temporal, spatial and cell-specific control of transgene expression in mice, the above mentioned transgenes were constructed based on the Tet-On gene regulation system. In order to yield spatially regulated transgene expression, rtTA (reverse tetracycline transactivator) was placed under the control of the SC-specific promoter for 2', 3'-cyclic nucleotide 3'-phosphodiesterase. Placement of genes under the control of the rtTA- P_{tight} system has been shown to display excellent dose-response characteristics, which allows not only a qualitative off-on transition but also a fine tuning of gene expression and the study of quantitative aspects of gene activity. The above mentioned transgenes constructed in this project were validated in Hek293T cells to ensure that they expressed in a tight and highly inducible manner. The transgene transfected cell lines when treated with doxycycline showed a dose-dependent expression of the gene of interest. Maximum gene induction was observed when treated with 0.5μg/ml doxycycline. In the absence of doxycycline, almost no or minimal gene expression was observed. The transgenes were

then excised out of the vector backbone for pronuclear microinjection. Once the transgenic mice are born, identified and validated, they shall be used for diabetic peripheral neuropathy research in the laboratory.

Acknowledgements

I joined Dr. Rick Dobrowsky's laboratory in the January of 2009 and my journey ever since has been more than wonderful. Dr Dobrowsky's mentoring, support and encouragement have played a pivotal role towards the accomplishment of this project. His utmost sincerity and dedication towards his profession will always be a benchmark as I embark on my career. He has been very patient, and has been forthcoming with suggestions and ideas whenever I hit a barrier. Most of all, I am very grateful to Dr. Dobrowsky for his persistent guidance and encouraging words which have instilled in me the confidence to pursue my dreams.

I would like to thank Dr. Staudinger for his valuable suggestions in this project. He has been very accommodating and has extended help whenever asked for. My special thanks to Dr. Davido for sparing his valuable time for my thesis and defense.

I would like to take this opportunity to thank my lab members; Liang, Melony, Chanel, Mike, Mac and Pan Pan, for their suggestions and warm presence. I thoroughly enjoyed the wonderful times we spent together. We all gelled very well, which created a conducive and healthy work environment. I have won great friends in this lab and hope to keep in touch with them in the long run.

I dedicate this work to my parents who have been my inspiration and are responsible for making me what I am today. Above all, I thank my husband for listening to my endless complaints about failing experiments, for those pep talks, for boosting my morale, and for giving me the unconditional love and support….Shyam, without you this would have been impossible.

I thank the Almighty for everything!

Contents

Table of Figures

I) INTRODUCTION

1.1) Mouse Transgenesis

An animal that gains new genetic information from the addition of foreign DNA is described as transgenic. The first transgenic animals were mice created by Rudolf Jaenisch in 1974[1]. Rudolf Jaenisch successfully managed to insert foreign DNA into the early-stage mouse embryos**,** where the resulting mice carried the modified gene in all their tissues[1]. Subsequent experiments in which leukemia genes were injected into early mouse embryos using a retroviral vector proved that the genes integrated not only to the mice themselves, but also to their progeny[2]. Transgenic animals have been produced in a variety of species with both commercial and scientific value[3]. Commercially they can be used for the preparation of recombinant proteins, protection of animals against disease, and introduction of new genetic traits into herds[2]. The generation of transgenic animals is essential for the in vivo study of gene function during development, organogenesis and aging[3]. It also permits the evaluation of therapeutic strategies in models of human diseases, as well as the investigation of disease progression in a manner not possible in human subjects[3].

Mice in particular offer the advantages of being relatively low in cost and having a short gestation time. Moreover, a well developed set of technologies exist for introducing genetic modifications into mice. The availability of genetically inbred strains and the relatively close evolutionary relationship of mice to humans are additional advantages[3]. Therefore, transgenesis in mice has been widely in use.

The discovery of new therapies for neurological disorders is predicated on the use of transgenic mice models, both to identify new therapeutic targets and to perform

preclinical trials of drugs before using them in patients[4]. Genetically engineered mice that recapitulate some of the features of human diseases can provide important new information about the neurobiology of these diseases[5].

1.2) Generation of Transgenic mice

The two most commonly used techniques for producing transgenic mice involves either the pronuclear injection of transgenes into fertilized oocytes or embryonic stem cell-mediated gene targeting[3]. Using **embryonic stem cell technology,** genetic modifications are first made in the embryonic stem (ES) cells. ES cell lines are derived from early-stage mouse embryos and can be maintained indefinitely in vitro in an undifferentiated state[3]. However, when injected back into an early-stage mouse embryo, they retain the capacity to mix with the endogenous cells of the embryo and contribute to the formation of all tissues in the developing mouse, including the germ cells[3] . Using a targeting vector that consists of a modified version of the endogenous gene, the gene of interest is integrated into the genome of the ES cells by homologous recombination. For efficient recombination to occur the targeting vector should include >3 kb of DNA homologous to the endogenous mouse gene[3]. Targeting vectors are also fitted with a gene conferring drug resistance or sensitivity for the selection of recombinant ES cells. Positive selectable markers like neomycin phosphotransferase (neo) resistance allow selection of ES cell clones that have incorporated the targeting vector. Figure 1 illustrates homologous recombination resulting in gene knockout.

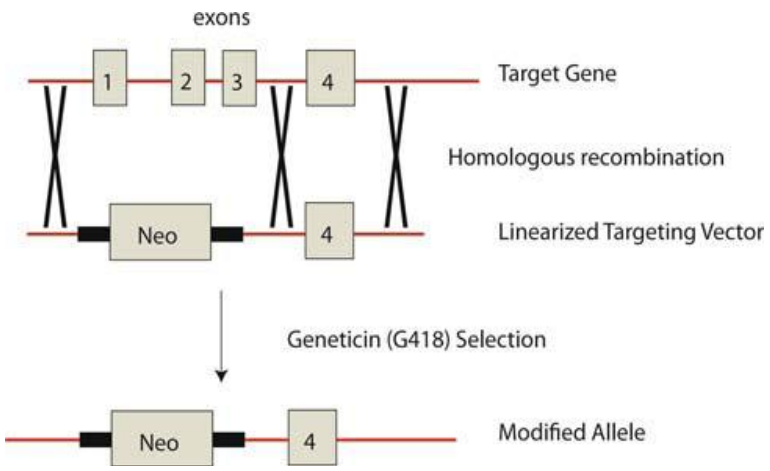

Figure 1: Homologous recombination

ES cells containing the recombined gene are then injected into a blastocyst-stage mouse embryo from which a chimeric mouse is generated. The resulting chimeras are bred and if successful integration of the ES cells into the germ line has occurred, the genetic modification will be propagated as part of the mouse genome creating stable lines harboring the specific genetic modification[6-7]. In contrast to pronuclear injection where multiple copies of the transgene insert randomly in the genome, the native mouse gene is modified in its normal chromosomal location using ES cell-based methods [3].

Pronuclear injection

Gordon et al. (1980) first described the introduction of a foreign gene into mice using pronuclear injection into oocytes. This approach has since been widely employed to study the molecular and cellular functions of many genes[8].

Transgene construction: When using pronuclear injection, a plasmid is constructed in which the gene/cDNA of interest is placed under the control of a heterologous promoter, whose choice depends upon where and when it is desired that the transgene be expressed. For a protein to be expressed, the cDNA must contain a translational start codon (ATG) with an upstream Kozak sequence [GCCGCC (G/A) NN]

to provide for ribosomal recognition of the mRNA start site and an in-frame translation stop codon (UGA, UAG, UAA) for translational termination[9]. Inclusion of an intron at the 5' or 3' end of the transgene allows splicing of the transgene[3]. Splicing generally results in more stable mRNAs and more efficient RNA translocation from the nucleus to the cytoplasm, which typically leads to better transgene expression[3]. Naturally occurring introns such as the simian virus 40 (SV40) intron or the rabbit β-globin intron, as well as artificial introns, can be used. In addition, eukaryotic transcriptional stop signals that include the poly (A)-addition sequence (AAUAAA) are usually positioned at the 3' end of the protein translation sequence. Termination sequences widely used include those from SV40, bovine growth home (BGH), and human growth hormone (HGH)[10]. Enhancer sequences are genetic control elements that act in position- and orientation-independent manners to control the level and pattern of gene expression[3]. Cell type specific expression of a transgene may be controlled by the inclusion of appropriate enhancer sequences. In order to prevent vector sequences from interfering with transgene expression, the transgenic cassette is typically excised from the plasmid backbone for microinjection[3].

Pro-nuclear DNA micro-injection is the oldest and most common method for transgenic mouse creation. A solution of the transgene is injected into fertilized oocytes with a microsyringe under a microscope[11]. These micro-injected oocytes are then transplanted in a surrogate mother. At birth the newborn are then tested for the presence of the transgene.

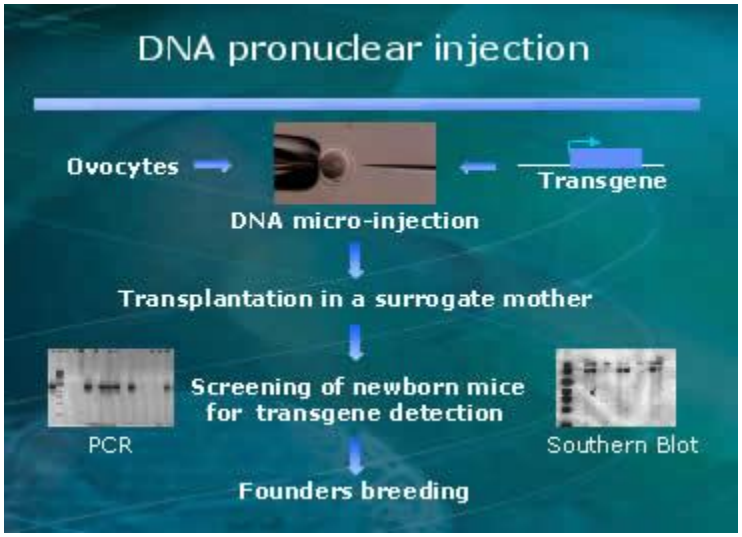

Figure 2: Pronuclear microinjection[11].

The foreign DNA integrates randomly and usually in the form of concatemers containing multiple copies of the original fragment (~70–100 kb). As there is no corresponding allele on the homologous chromosome opposite the integration site, these mice are most appropriately referred to as ‘‘hemizygous’’ rather than ‘‘heterozygous’’[3]. The number of integrated transgenes (the transgene copy number) is generally inversely proportional to fragment size. Therefore, with larger DNA fragments, fewer copies will typically integrate. Due to the random nature of transgene integration following pronuclear microinjection, position site-dependent effects may alter transgene expression. These effects may produce transgene silencing, modify the cell and tissue specificity of the transgene or affect overall level of expression.

Inclusion of insulator sequences can minimize insertion site effects. Chromatin insulator elements are DNA sequences that together with their binding proteins block interactions between adjacent chromatin domains. These elements establish genomic barriers that protect DNA sequences from the effects of neighboring sequences[3]. Among the insulator sequences that have been studied, the 5’HS4 chicken

β-globin (a constitutive DNAse I-hypersensitive site 5’ of the chicken beta-globin locus) and the mouse tyrosinase locus control region (LCR) insulator elements have both been shown to reduce the variability of transgenic expression when introduced either 5’, or 5’ and 3’ relative to heterologous transgenes[12-14].

Inducible transgene expression: In most gene therapies the transgene is delivered under the control of a promoter that allows constitutive expression[15]. In these cases, no control on the level or the timing of transgene expression can be exerted. However, there are numerous cases in which controlling the transgene expression "from outside" would be preferable[15]. For instance, if high levels of the transgene are toxic, quantitative control of its expression should prevent adverse side effects. Moreover, if the window of action of the transgene is narrow, temporal control could allow delivery of the product at the right moment[15]. The study of gene function in complex genetic environments such as mammalian cells would greatly profit from systems that would allow stringent control of the expression of individual genes[16]. Ideally, such systems would not only mediate an "on/off" situation of gene activity but would also permit limited expression at a defined level[16]. Attempts to control gene activity by various inducible eukaryotic promoters responsive to, for example, heavy metal ions[17-18], heat shock[16], or hormones have generally suffered from leakiness of the inactive state. In search of regulatory systems that do not rely on endogenous control elements, Gossen and Bujard developed the tet regulatory system.

1.3) Tet regulatory system

This system is based on the regulatory elements of the Tn 10-specified (transposable element) tetracycline-resistance operon of E. coli[19]. In E. coli, the tetracycline repressor (tetR) is inactivated by the interaction with tetracycline. Due to this, it is unable to bind to the tet operator sequences (*tetO*) located within the promoter region of the operon. This leads to the transcription of the genes of the tetracycline resistance operon. In the absence of tetracycline, tetR blocks transcription of these genes by binding to the tet operator (*tetO*) sequences. The design of the "Tet-on" and "Tet-off system is the fruit of Dr. Gossen and his colleagues[16, 20]. These systems have two critical components; 1) the response plasmid containing the gene of interest and the tetracycline response element (TRE); 2) the regulatory protein based on tetR.

The response plasmid expresses the gene of interest under the control of **TRE**. The TRE consists of seven direct repeats of a 42bp sequence containing the tetO (tetracycline operator sequences), located just upstream of the minimal CMV promoter (P_{minCMV}). P_{minCMV} lacks the strong enhancer elements normally associated with the CMV immediate early promoter[21]. As these enhancer elements are missing, there is low background expression of the gene of interest from the TRE in the absence of binding by the tTA or the rtTA[21].

In the **Tet-off system**, the 37-kDa regulatory protein is a fusion of amino acids 1-207 of tetR and the C terminal (127a.a.) of the Herpes simplex virus VP16 activation domain[22]. The VP16 domain converts the tetR from a transcriptional repressor to a transcriptional activator, and the resulting hybrid protein is known as the tetracycline-controlled transactivator (tTA)[21]. Doxycycline interacts with tTA and

inactivates it (tetR inactivation). In the absence of doxycycline, tTA is capable of binding to TRE. Being a transactivator, it interacts with TRE and helps transcribe the gene of interest only after the removal of doxycycline (Figure 3a).

The **Tet-on system** is similar to the Tet-off system, but the regulatory protein is based on a "reverse" tetracycline repressor (rtetR) which was created by four amino acid changes in tetR[20] ($Glu^{71} \rightarrow Lys^{71}$, $Asp^{95} \rightarrow Asn^{95}$, $Leu^{101} \rightarrow Ser^{101}$, and $Gly^{102} \rightarrow Asp^{102}$). The resulting hybrid protein after the addition of the VP16 domain is called the reverse tetracycline transactivator (rtTA). Due to the amino acid changes in tTA, the resultant rtTA can bind the TRE only in the presence of doxycycline. Thus, rtTA interacts with TRE and causes gene transcription in the presence of doxycycline (Figure 3b).

The pTRE-Tight vector series (Clontech) used in this study contains a modified TRE (TRE_{mod}) upstream of an altered minimal CMV promoter ($P_{minCMV\Delta}$), resulting in further reduced basal expression of the gene of interest[21]. pTRE-Tight can fully minimize background expression in certain cell lines, and is especially useful in cases where background expression is unacceptable[21]. Thus, when the cells contain the two components of this system; the regulatory plasmid (containing the rtTA or the tTA) and the response plasmid (gene of interest under the control of TRE), the gene of interest is only expressed upon binding of the rtTA or tTA to the TRE.

pTet-On Advanced expression system: The pTet-On-Advanced vector (Clontech) expresses an improved version of the reverse tetracycline-controlled transactivator protein (rtTA), called rtTA-Advanced (Figure 3c). It is more sensitive to doxycycline (Dox) and yields lower background expression than the original rtTA[21]. The rtTA-Advanced protein is a fusion of amino acids 1-207 of the mutant tetracycline-

repressor (rtetR) and 39 amino acids containing three minimal “F”- type transcriptional activation domains from the VP16 protein of the herpes simplex virus[21]. It is fully synthetic, lacks cryptic splice sites, and is codon optimized for stable expression in mammalian cells[21].

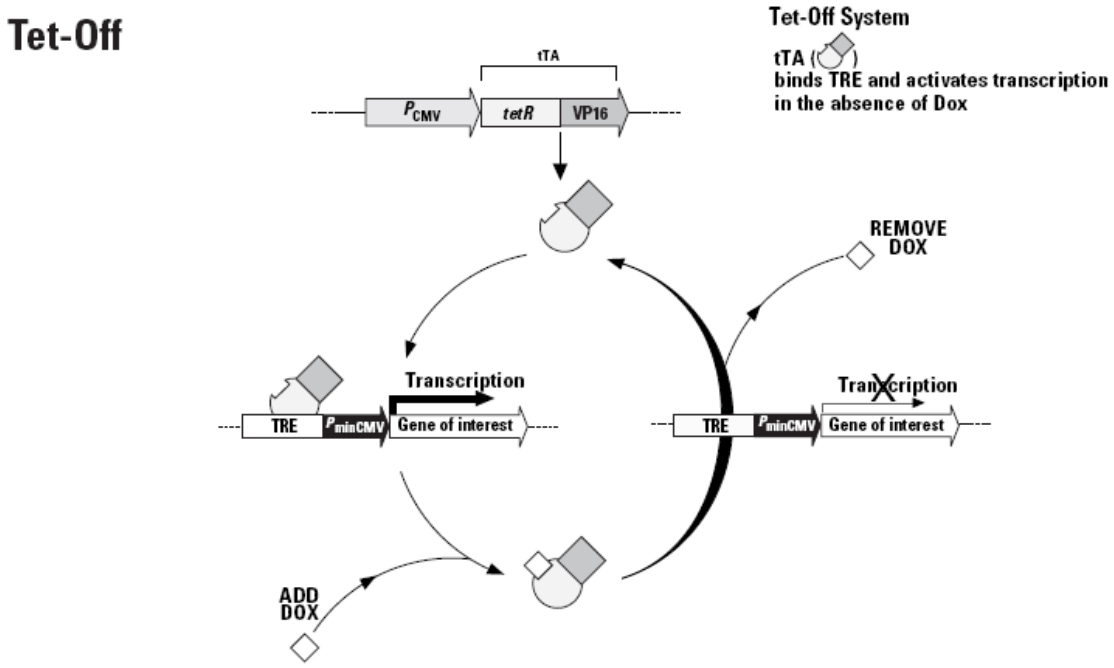

Figure 3a[21].

Tet-On

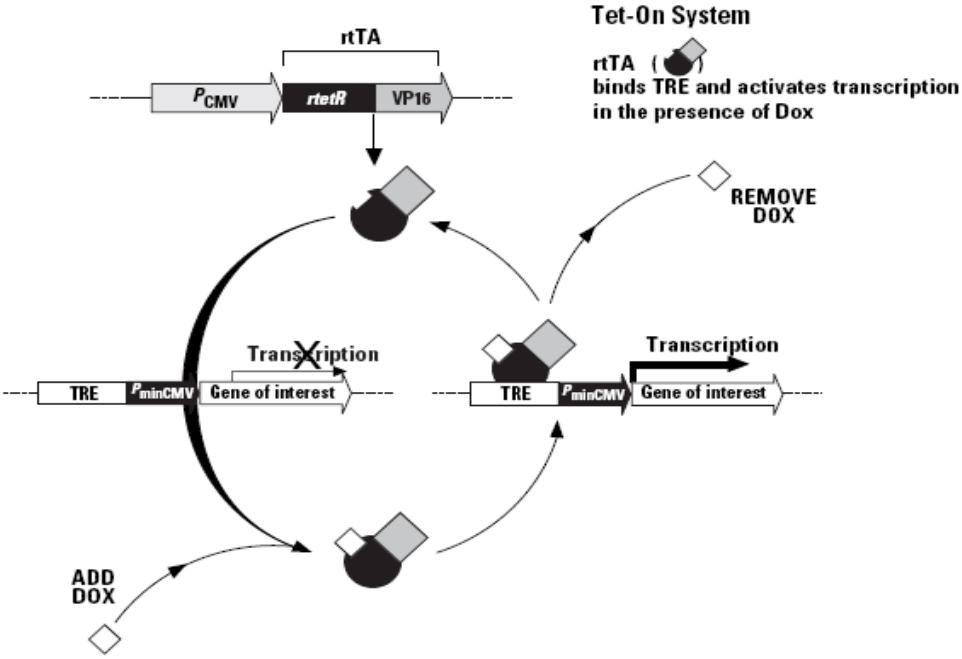

Figure 3b[21].

Figure 3: Tet regulatory system

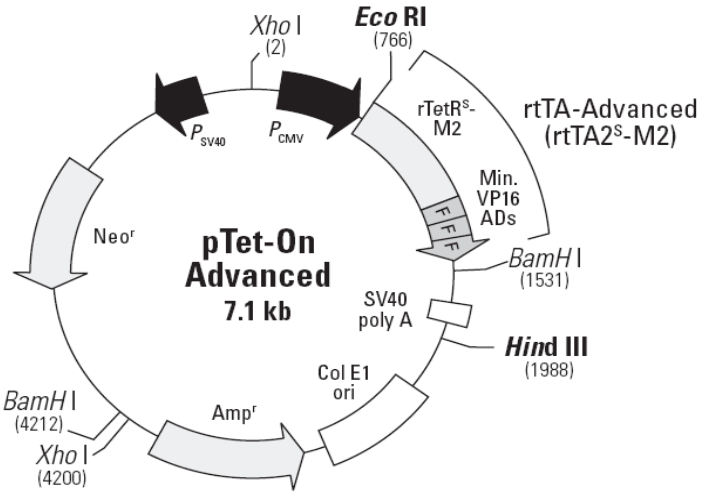

Figure 3c[21].

Figure 3a and 3b are schematics of gene regulation in the Tet-Off and Tet-On Systems respectively. Figure 3c is the vector map of the pTet-On Advanced vector provided by Clontech.

Tet-Off vs Tet-On Systems:

When properly optimized, both systems give tight on/off control of gene expression, regulated dose-dependent induction with similar kinetics of induction, and high absolute levels of gene expression[21]. Thus, for most purposes, there is no inherent advantage of using one system over the other[21]. With the Tet-Off system, it is necessary to keep tetracycline (Tc) or doxycycline (Dox) in the medium to maintain the native (off) state. Due to the relatively short half-lives of Tc and Dox, one must add them to the medium at least every 48 hours to suppress the expression of the gene of interest. Conversely, in the Tet-On system, Dox is added to the medium only when induction is required.

The Tet-On system is only responsive to Dox, not Tc [20]. In contrast the Tet-Off systems respond equally well to either Tc or Dox[21]. Dox has been recommended for all Tet Systems in part because a significantly lower concentration of Dox is required for complete activation or inactivation (0.01-1μg/ml Dox vs 1-2 μg/ml Tc)[21]. Moreover, Dox has a longer half-life (24 hours) than Tc (12 hours)[21].

1.4) Analysis of transgenic mice

Genomic DNA isolated from a small piece of tail or ear tissue is used for the identification and analysis of transgenic mice. The analysis must establish the presence of the transgene, the zygosity, the transgene copy number, and whether transgene rearrangement or deletion has occurred[3]. Polymerase chain reaction (PCR) and/or Southern blotting can be used to detect the presence of the transgene. Transgene copy number can be determined using Southern blotting or real-time quantitative PCR

(qPCR) based assays. Southern blotting can also be used to detect major rearrangements of the transgene. Moreover, fluorescence in situ hybridization (FISH) can be used to microscopically visualize transgenic integration. This technique allows detection of transgenic animals[23], determination of the chromosomal integration site[24], the local chromatin structure, and the effect of the integration site on gene expression[25].

For the next level of analysis, quantitative RT-PCR (qRT-PCR) is usually the technique of choice. It helps to determine, the pattern and level of transgene transcription or, the absence of expression in animals in which a gene target has been silenced or deleted[3]. Finally, characterization should include analysis of the protein product and its level of expression, which can be correlated with any phenotype that the transgenic mouse exhibits[3]. Western blotting, enzyme-linked immunosorbent assays (ELISA), radioimmunoassay (RIA), and immunohistochemistry are some of the techniques that could be used for the above.

1.5) PROJECT OUTLINE

Aim: To generate three different bi-transgenic mouse models for diabetic neuropathy research.

Summary: The transgenes were constructed based on the Tet-On gene regulation system. Each model is represented by two transgenes; the regulatory transgene and the response transgene. The regulatory transgene contains the rtTA-advanced cDNA under the control of the promoter for 2', 3'-cyclic nucleotide 3'-phosphodiesterase (CNPase), which ensures the transgene's expression in myelinating Schwann cells. The

response transgene contains the gene of interest under the control of the P_{tight} Tet-responsive promoter (Clontech).

1) Cnpase-rtTA; P_{tight} -DN-ErbB4
2) Cnpase-rtTA; P_{tight} -dn-Ubc9
3) Cnpase-rtTA; P_{tight} -Cre

The above transgenes are discussed in more detail in the ensuing sections. In order to validate the expression of the transgene pairs, these were tested on cell lines. The transgene transfected cell lines when treated with doxycycline showed a dose-dependent expression of the gene of interest. Maximum gene induction was observed when treated with 0.5μg/ml doxycycline. In the absence of doxycycline, almost no or minimal gene expression was observed. In vitro, the transgenes expressed in a tight and highly inducible manner.

The transgenes were excised out of the vector backbone for pronuclear microinjection. In order to genotype the transgenic mice, when born, PCR conditions were standardized using the primers designed against the transgenes.

1.6) Diabetic Peripheral Neuropathy

Peripheral neuropathy, also called distal symmetric neuropathy or sensorimotor neuropathy, is the nerve damage in the arms and legs[26]. Diabetic peripheral neuropathy (DPN) is a common complication of diabetes[27]. About 60% to 70% of all people with diabetes will eventually develop peripheral neuropathy, although not all suffer pain[26]. Symptoms of peripheral neuropathy may include

- numbness or insensitivity to pain or temperature
- a tingling, burning, or prickling sensation

- sharp pains or cramps
- extreme sensitivity to touch, even light touch
- loss of balance and coordination

Although hyperglycemia is the definitive cause of DPN, the vascular, glial, and neuronal damage that underlies the progressive axonopathy in DPN has a complex biochemical etiology involving oxidative stress, protein glycation, protein kinase C activation, polyol synthesis, and the hexosamine pathway[27].

The pathology of peripheral neuropathy follows three basic patterns: Wallerian degeneration, distal axonopathy, and segmental demyelination[28]. Demyelinating neuropathies are those in which the Schwann cells (SCs), which form myelin, are primarily affected and migrate away from the nerve[28]. This process causes the insulating myelin of axon segments to be lost, and conduction of nerve impulses down the axon is blocked. Though demyelination occurs in human neuropathy, it is not a hall mark of neuropathy in rodents[29]. Thus, it is important to study the mechanisms affecting myelination, to throw light on the pathophysiological progression of DPN. Our strategy has been to use the dominant negative transgenes, with SC specific expression, to investigate the role of these target genes in DPN.

The following sections shall describe the CNPase promoter and the dominant negative constructs.

1.7) 2',3'-cyclic nucleotide 3'-phosphodiesterase

The enzyme 2',3'-cyclic nucleotide 3'-phosphodiesterase is an oligodendroglial protein comprising 4-5% of the total protein of isolated CNS myelin[30].

It is named for its ability to catalyze the phosphodiester hydrolysis of 2',3'-cyclic nucleotides to 2'-nucleotides, though a cohesive understanding of its specific physiologic functions are still ambiguous[31]. CNPase's catalytic core consists of three alpha-helices and nine beta-strands[32].

CNPase is found mainly in the central nervous system of vertebrates, especially of amphibia and higher vertebrates[33]. It is the first of the major myelin-related proteins to appear in the developing brain[34]. The deposition of this protein in brain parallels the developmental accumulation of myelin and thus has served as a useful biochemical marker for myelin membrane in vitro[35-37]. It is relatively abundant in myelinating oligodendrocytes and Schwann cells [38-39] and is found to be localized in the cytoplasm of non-compact myelin[31]. It is also present at low levels in some other non-neural tissues, notably, lymphoid tissues and photoreceptor cells[38-39].

Several functional studies have suggested possible functions of CNPase. Isoprenylation of rat CNPase demonstrated that the C-terminal domain of CNPase is important for membrane binding and localization[40]. Overexpression of CNPase in transgenic mice induced aberrant myelination[41]. CNPase has been implicated in several diseases: Down's syndrome[42], Alzheimer's disease[42-43], and multiple sclerosis[44]. Recent studies on CNPase-knockout mice revealed that disruption of the CNPase gene causes hydrocephalus and premature death[45]

There are two isoforms of this protein: CNPase1 (46 kDa) and CNPase2 (48 kDa)[46]. CNPase2 differs structurally from CNPase1 by having a 20-amino acid extension at the N-terminus[47-49]. Molecular genetic studies have shown that the two CNPase isoforms are encoded by a single CNPase gene[48, 50]. Analysis of the structure

of CNPase cDNAs and genomic regions from rat, mouse, bovine, and human suggest that the overall organization of the gene is very similar in all species[48-49, 51-52]. The gene is composed of four exons[46]. Two AUG codons responsible for the translation initiation of CNPase2 and CNPase1 polypeptide isoforms are located in the first and second exons, respectively. Separate promoter regions control the expression of CNPase1 and CNPase2 transcripts[46]. The CNPase1 mRNA (2.6 Kb) is transcribed from the proximal promoter (P1 in Figure 4) and contains only the open reading frame for CNPase1 protein[46]. Transcription from the distal promoter (P2 in Figure 4), followed by an additional splicing event within the non-coding region of exon 1, produces the CNPase2 mRNA (2.4 Kb). The CNPase2 mRNA contains both AUG initiation codons and has the coding capacity for the translation of both CNPase isoforms (Figure 4).

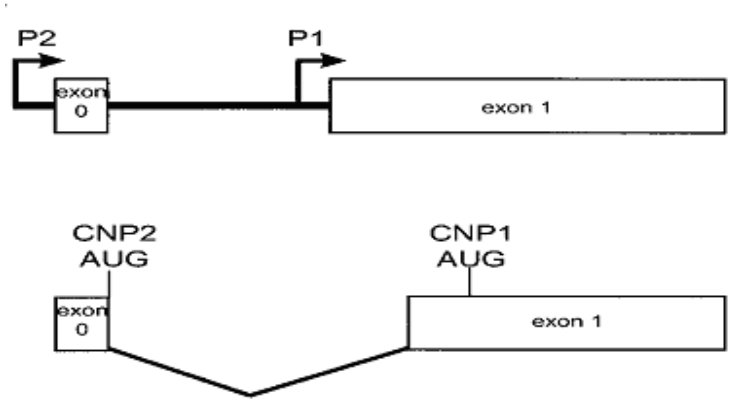

Figure 4. ***Alternative splicing of exon 0 to exon 1 in the CNPase gene***[46]**.**

Findings suggest that the CNPase promoter could be a valuable tool for targeting expression of other heterologous genes in the CNS for the purpose of studying brain development or for developing expression systems in gene therapy [53]. Transgenic mice are one of the best overall gene function assay systems for the characterization and

identification of regulatory elements[53]. This approach was used to characterize the properties of the CNPase promoter.

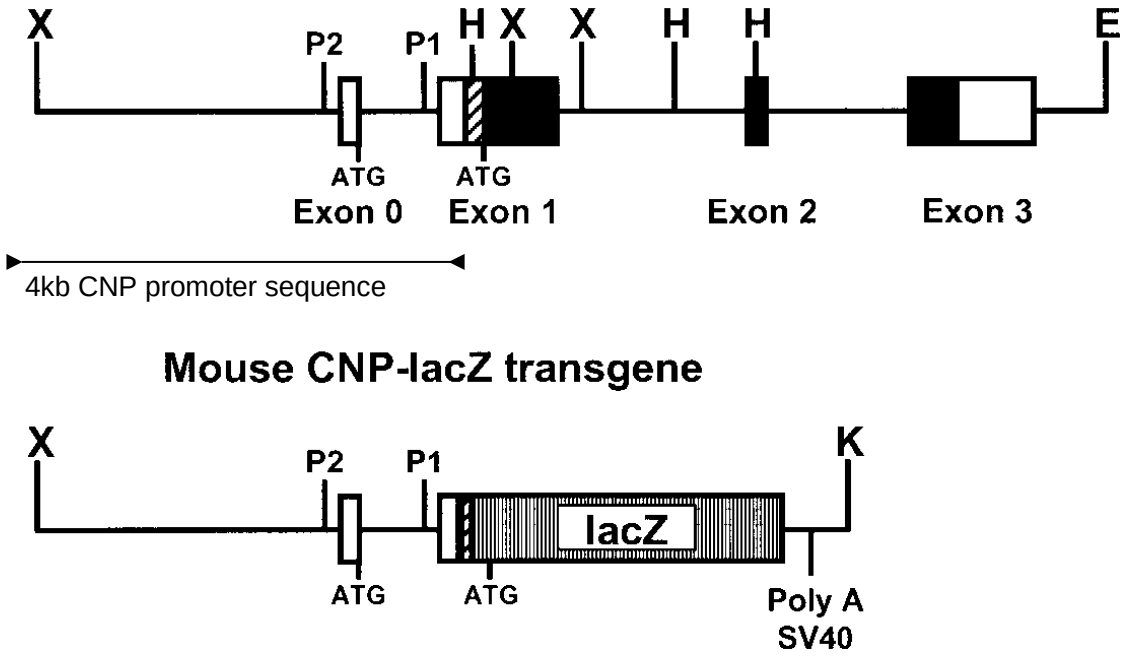

Figure 5: Structure of the CNPase gene and the CNPase-lacZ transgene construct[53].

Shown above is the structure of the CNPase gene and the CNPase-lacZ transgene construct. The relevant restriction endonuclease sites are indicated as *Xba*I (X), *Hin*dIII (H), *Eco*RI (E), and *Kpn*I (K). P1 and P2 indicate the two TATA-box sequences of CNPase1 and CNPase2 promoters, respectively[53]. Solid boxes are common coding regions of both CNPase1 and CNPase2; open boxes are noncoding regions; hatched boxes contain the sequence corresponding to the 20–amino acid extension at the N-terminus of CNPase2[53]. The XbaI site at the leftmost end in Figure 5 is 4kb upstream from the cap site of CNPase1. The sequence between this XbaI site and the HindIII site in exon1 contains both CNPase1 and CNPase2 promoter core elements[53]. Linking the

lacZ reporter gene (along with the SV40 polyadenylation signal) downstream of the 4kb promoter sequence generated the CNPase-lacZ transgene construct[53].

It has been demonstrated that the CNPase-lacZ fusion gene contains sufficient information to allow spatial and temporal regulation of lacZ expression in a manner similar to endogenous CNPase expression[53]. CNPase promoter driven lacZ expression is shown to be strongest in neural tissues; in non-neural tissues, only testis and thymus are reported to have low levels of expression[53]. Moreover, it has been demonstrated that in the brain, the CNPase-driven lacZ expression is strongest in the oligodendrocytes[53]. The distribution and the level of transgene expression in these transgenic mice agree well with the level of endogenous CNPase activity[53].

The transgene constructs developed in this project have incorporated the CNPase promoter to drive the expression of two dominant negative genes, namely; DN-ErbB4 and dnUbc9

1.8) DN-ErbB4

The ErbB protein family or epidermal growth factor receptor (EGFR) family is a family of four structurally related receptor tyrosine kinases[54] namely:

- ErbB-1, also named epidermal growth factor receptor (EGFR)
- ErbB-2, also named HER2 in humans and neu in rodents
- ErbB-3, also named HER3 and
- ErbB-4, also named HER4

All the above family members have in common an extracellular ligand-binding domain, a single membrane spanning region and a cytoplasmic protein tyrosine

kinase domain[55]. A family of ligands (EGF-related peptide growth factors) bind the extracellular domain of ErbB receptors leading to the formation of both homo- and heterodimers[55]. Dimerization consequently stimulates the intrinsic tyrosine kinase activity of the receptors and triggers autophosphorylation of specific tyrosine residues within the cytoplasmic domain. These phosphorylated residues serve as docking sites for signaling molecules involved in the regulation of intracellular signaling cascades[55]. Ultimately, downstream effects on gene expression determine the biological response to receptor activation.

The neuregulins (NRGs 1–4) have been identified as a family of EGF-domain containing molecules that serve as ligands for the ErbBs[56-65]. In the central nervous system (CNS), NRG1/ErbB signaling has been implicated in a broad range of roles, including myelination, neuronal migration, axonal pathfinding, and synaptic function[66-68]. Activation of ErbB receptors through tyrosine phosphorylation has been shown to regulate cell proliferation, migration and differentiation in different neural systems[69-71]. The involvement of ErbB signaling in the above mentioned biological processes makes it important to explore this signaling pathway further.

In order to elucidate the role of ErbB signaling, and to determine whether the disruption of this pathway produces defects related to disease, a construct containing a truncated version of the ErbB4 receptor has been generated. This dominant negative ErbB4 receptor (DN-ErbB4) lacks most of the intracellular domain, including the tyrosine kinase domain and the tyrosine phosphorylation sites[72]. These domains and sites have been replaced by a FLAG epitope tag[72]. The protein expressed by the DN-ErbB4 construct is ~130kDa[72]. This construct blocks all neuregulin signaling by

binding NRG ligands and preventing them from binding to endogenous ErbB3, and ErbB4[73]. Thus, the over-expression of DN-ErbB4 completely blocks ErbB2, ErbB3, and ErbB4 receptor signaling[72, 74-75].

Some reports indicate that increased ErbB4 expression or signaling is associated with tumorigenesis. ErbB4 over-expression has been observed in a variety of cancers, including tumors of the thyroid, breast, and gastrointestinal tract[76-77]. NRG1/erbB4 signaling is genetically linked to schizophrenia and bipolar disorder[78]. Moreover, mice with reduced levels of NRG1 or erbB4 exhibit behavioral alterations relevant to mental illness[79-82]. Although the evidence linking this pathway and psychiatric disorders is strong, the mechanisms by which it contributes to these diseases remain unknown[73]. NRG1-erbB signaling is important in neurons, astrocytes, and oligodendrocytes (OLs), but the specific cell types through which altered NRG1-erbB signaling contributes to these psychiatric disorders is undefined[73]. Efforts to elucidate ErbB4 function have been hampered by many factors. There are no known agonists or antagonists specific to the ErbB4 receptor[83]. All of the peptide hormones of the EGF family that are capable of binding ErbB4 also bind at least one other ErbB family member[83]. Upon NRG binding, erbB receptors form homo- and heterodimers and become active.

It has been hypothesized that expression of DN-ErbB4 should block the activation of all NRG receptors[72]. This would help to study the role of these receptors in various biological processes. Transgenic mice have been generated that express dominant negative ErbB4 receptor (DN-erbB4) under the control of the CNPase promoter [74]. The CNP promoter ensures tissue specific expression of DN-ErbB4, which in turn

has helped to reveal the ErbB function in specific cell types and has been able to throw more light on the ErbB signaling network on the whole. However, this animal model is limited by its reliance on the endogenous regulation of CNPase promoter activity. Our transgene constructs will permit a temporal and spatial control over the DN-ErbB4 expression since it is induced in the mice only in the presence of Dox.

CNPase-rtTA; TRE-DN-ErbB4 bi-transgenic mouse model for DPN research:

Evidence supports that pathologic activation of ErbB2 is sufficient to induce SC dedifferentiation and demyelination[84]. Additionally, studies have shown that endogenous proteins, like caveolin-1, that regulate the activity of ErbB2, may influence the development of certain aspects of sensory neuropathies[27]. Considering the importance of the ErbB2 receptor in the development of sensory neuropathies and the contribution of the NRG1-ErbB signaling for generating myelin with normal thickness, it is essential to determine if inhibiting the neuregulin signaling in SCs can increase demyelination in DPN.

Knock-out (KO) mice failed to provide information about the roles of NRG1–erbB signaling in the postnatal period, the time at which myelination occurs, owing to their early lethality[74]. Moreover, because most of the analyses were performed in animal models with reductions (hypomorphs) rather than complete elimination of erbB signaling, the contributions of erbB signaling to myelin formation remained poorly defined[74].

To elucidate the role of erbB receptor signaling in myelinating Schwann cells with respect to DPN, this project aims to generate bitransgenic (Tg) mice with the transgenes; CNPase-rtTA and TRE-DN-ErbB4. The CNPase promoter would ensure the

expression of the dominant negative ErbB4 only in myelinating Schwann cells, wherein, Dox would ensure that the DN-ErbB4 expresses in a tight and highly inducible manner. Expression of DN-erbB4 may completely block erbB2, erbB3, and erbB4 receptor signaling[72, 74-75]. Thus, once diabetes is induced in such mice, it would enable researchers to study the effect of impaired neuregulin signaling on myelination with respect to the progression of DPN.

1.9) dnUbc9

The *ubc9* (Ubiquitin-like protein SUMO-1 conjugating enzyme) gene of the yeast Saccharomyces cerevisiae (Sc*ubc9*) is an essential gene which is required for cell cycle progression and is involved in the degradation of S phase and M phase cyclins. A human homolog of Sc*ubc9* (termed h*ubc9*) has been identified which shares a very high degree of amino acid sequence similarity with ScUBC9[85]. Genetic complementation experiments reveal that hUBC9 can substitute for the function of ScUBC9 required for cell cycle progression[85]. The h*ubc9* gene is located at the chromosomal position 16p13.3[86] and encodes a transcript of 1.3 kb[85]. The open reading frame of this gene encodes a protein of 158 amino acids with a predicted molecular size of 18kDa[85].

Ubc9 is highly conserved across species and is expressed ubiquitously, but the expression level differs among various tissues[87]. This enzyme is a ubiqutin conjugating enzyme (E2 enzyme) required for small ubiqiutin-related modifier (SUMO) conjugation or sumoylation. Sumoylation is the covalent attachment of SUMO proteins to specific lysine residues of target proteins.

Modification by SUMO uses the same chemical steps of conjugation as other ubiquitin(-like) proteins (Figure 6), starting with an ATP-dependent activation step by an E1 enzyme (ubiquitin-activating enzyme) to form a thioester bond between an active site cysteine and the C terminus of the ubiquitin(-like) protein[88]. In the next step, this thioester is transferred to a cysteine on an E2 conjugating enzyme. From the E2 thioester, the ubiquitin(-like) moiety is transferred to a lysine on the target protein[88]. Thus, the E2 enzymes function by accepting the ubiquitin(-like) protein through a thioester and then transferring it to form an isopeptide bond with the target lysine[88]. This E2-mediated transfer reaction can be catalyzed by E3 enzymes [89-91], but these seem to function mostly by providing a scaffold for the reactants, thus leaving the actual transfer reaction to the E2 protein[92-94].

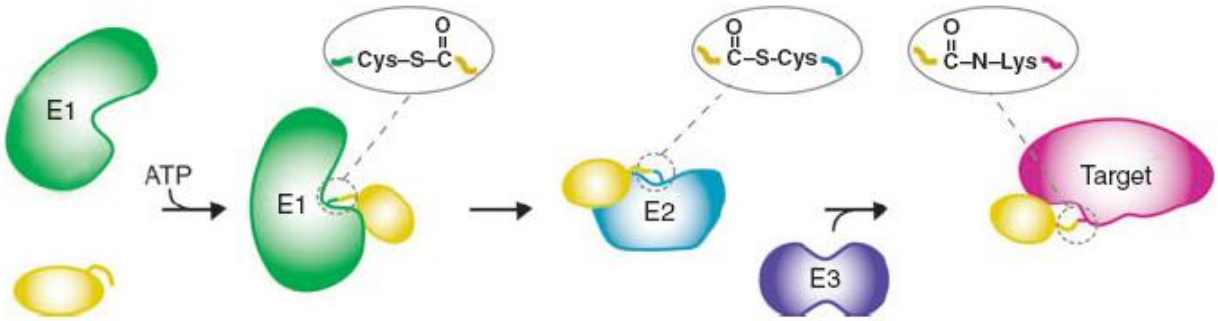

Figure 6: Scheme for Sumoylation[88].

Among the structurally conserved E2s, the SUMO E2 Ubc9 is special because it preferentially targets a ΨKXD/E consensus site[88]. Ubc9 is the sole E2-conjugating enzyme required for protein sumoylation[95]. Sumoylation is a post-translational modification required for various cellular processes, such as nuclear-cytosolic transport, transcriptional regulation, apoptosis, protein stability, response to stress, and progression through the cell cycle[96]. In addition, it has been demonstrated

that sumoylation of DNA topoisomerase I plays a critical role in DNA metabolism and transcription. Since Ubc9 is critical for sumoylation, it plays an important role in the above mentioned biological processes through sumoylation. Ubc9 has also been implicated in apoptosis and DNA repair, because it interacts with proteins such as p53 and Rad51[97-100]. Therefore, it would be useful to further explore the cellular functions of Ubc9.

In yeast and higher eukaryotic cells, gene disruption of Ubc9 has been reported to be lethal[101-102]. Its involvement in regulating several critical pathways hampers researchers from knocking down this gene in order to study its functions. A substitution mutant of h*ubc9* (Cys→Ser at codon 93, TGC→AGC) was generated using PCR-mediated, site-directed mutagenesis[85]. This mutant exhibits a dominant inhibitory effect on the endogenous Ubc9[103] and hence provides a useful tool to study the cellular functions of Ubc9.

Studies have indicated that sumoylation has a role in human disease pathogenesis. Indeed, proteins that have key roles in several human disease states, including huntingtin, ataxin-1, tau, a-synuclein, DJ-1 (also called Parkinson's disease 7 [PARK7]), and superoxide dismutase 1 (SOD1), are targets of SUMO modification[104]. Ubc9 being the sole E2 conjugating enzyme required for sumoylation, has thus been implicated in the pathogenesis of the diseases associated with the above mentioned proteins. Increased Ubc9 levels are found in several human cancers and Ubc9 overexpression can increase cancer cell growth[104].

A Ubc9-DN transgene under the control of the Tet-regulatory system would be able to overexpress Ubc9-DN in the presence of Dox, thus exhibiting a dominant

inhibitory effect on the endogenous Ubc9. Such a transgenic mouse model would be able to elucidate the role of Ubc9 in the pathogenesis of several human diseases.

CNPase-rtTA; P_{tight} -dnUbc9 bi-transgenic mouse model for DPN research:

Apart from neuregulin signaling, the heat shock response too has an effect on myelination. Evidence from studies underscore the therapeutic potential of heat shock proteins for demyelinating neuropathies[105]. It has been reported that EC137, a small-molecule inhibitor of HSP90, effectively enhances chaperone levels (HSP27, HSP70 and αB-crystallin) and improves myelination by SCs from neuropathic mice[105]. However, the precise molecular mechanism by which inhibition of HSP90 aids myelin formation remains unclear[105].

The transcription of the genes of heat shock proteins is mediated by heat shock transcription factor 1 (HSF1), which exists in a non-DNA-binding form in the absence of stress[106]. Heat shock converts HSF1 to the trimeric DNA binding-form that then interacts with promoters of heat shock protein (hsp) genes to up-regulate transcription[107-108]. It has been demonstrated that heat stress causes HSF1 sumoylation, and that this modification activates the DNA binding ability of HSF1[109]. Hence, sumoylation could be playing a pivotal role in the generation of heat shock proteins through HSF1 activation. The role of sumoylation in the generation of HSPs, together with the evidence that the pharmacological induction of HSPs improves myelination in neuropathic models, implies that sumoylation could be involved in the progression of DPN.

Groups have reported that hyperglycemia increases mitochondrial fission in both in vitro and in vivo models of diabetic neuropathy[110]. Knockdown of the dynamin-related protein 1 (Drp1), a key regulator of mitochondrial fission, rescues mitochondria from short-term glucotoxicity in vitro[110]. Despite the short-term beneficial effects of Drp1 knockdown, its role in the long-term development of diabetic neuropathy remains to be defined[110]. Recent advances in understanding the role of the fission protein Drp1 in mitochondria function indicate that Drp1 may be a central regulator of neuropathies[111-113]. Thus, it is of relevance to explore the mechanisms through which Drp1 contributes to the progression of DPN. Recent data suggests that Drp1 interacts with the SUMO-conjugating enzyme Ubc9 *via* multiple regions and demonstrates that Drp1 is a direct target of SUMO modification[114]. Expression of the construct dn-Ubc9 exerts a dominant inhibitory effect on the UBC9 enzyme[103] and is thus capable of interfering with the sumoylation of Drp1. Such interference would throw light on the contribution of Drp1 sumoylation towards DPN.

The above mentioned evidence led to the hypothesis that sumoylation could be involved in the progression of DPN. In order to study the role of sumoylation in SCs with respect to DPN, this project aims at generating a bi-transgenic mouse model (CNPase-rtTA; P_{tight} -dn-Ubc9) that expresses the dominant negative Ubc9 construct in myelinating SCs in a temporally regulated manner. In such mouse models, the expression of the dnUbc9 transgene would interfere with sumoylation, thus permitting researchers to assess the role of this post-translational modification in DPN.

Apart from creating transgenic mice that express dominant negative genes, in order to elucidate the involvement of plausible mechanisms in the progression of DPN, gene knockout technology would also prove to be invaluable in understanding the pathogenesis of DPN. Though invaluable in the study of gene function in vivo, this technology may lead to embryonic lethal phenotypes. In order to circumvent this limitation, methods have been developed allowing in vivo gene inactivation at defined time points. The most widely used approach developed to date makes use of the Cre/loxP recombination system[115].

1.10) Cre Recombinase

Site-specific recombinases from the lambda integrase family of enzymes catalyze DNA rearrangements that are critical for a variety of important biological functions[116]. Cre recombinase from bacteriophage P1 is one such enzyme. *cre* gene, short for cyclization recombination[117], encodes a 38kDa site-specific DNA recombinase[116] logically named Cre. Its roles in the P1 life cycle are thought to include cyclization of the linear genome and resolution of dimeric chromosomes formed following DNA replication as a result of homologous recombination[118]. The monomeric Cre protein contains amino terminal, linker and carboxy terminal domains[119]. The amino terminal domain comprises five alpha helices whereas the carboxy terminal domain contains nine alpha helices[119]. The carboxy terminal domain harbors the Cre recombinase active site, consisting of Arg^{173}, His^{289}, Arg^{292}, Trp^{315}, and the phosphate attacking Tyr^{324}.

The stable introduction of DNA into mammalian cells by microinjection generally results in seemingly random integration of the DNA into the genome[120-123]. Homologous recombination events between the chromosome and introduced DNA's do occur, but at low efficiency[124-125]. As an alternative and complementary approach to effecting specific homologous recombination events in eukaryotes, the prokaryotic Cre-lox site-specific DNA recombination system has been studied. Since being discovered, the bacteriophage's recombination strategy has been developed as a technology for genome manipulation and successfully applied in mammalian cell cultures, yeasts, plants, mice, and other organisms[126].

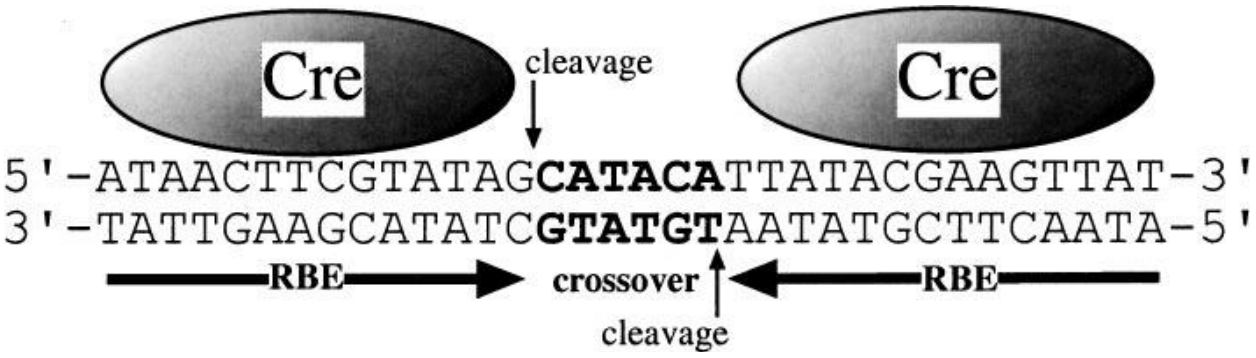

Figure 7: Cre recombinase structural elements[116].

Cre recombinase mediates intramolecular and intermolecular site-specific recombination[127]. The 34 base pair DNA sequences where recombinase binding and strand exchange take place are named *loxP* in the Cre recombinase system[115]. These sites are composed of two 14bp recombinase binding elements (RBEs) arranged as nearly perfect inverted repeats surrounding a 6bp central strand exchange or crossover region (Figure 7)[116]. Two recombinase subunits bind to each core site (one to each RBE) with

a high level of cooperativity[128-129]. On binding the palindromic halves of the loxP sites, the recombinase molecules form a tetramer, thus bringing together the two loxP sites and causing recombination within the spacer area of the loxP sites[115]. Figure 8A shows the target DNA flanked by loxP sites. The Cre enzyme binds to these sites and cuts them into palindromic halves[130]. This results in the excision of the target DNA (Figure 8B). The remaining palindromic halves of the loxP sites are then spliced together[130].

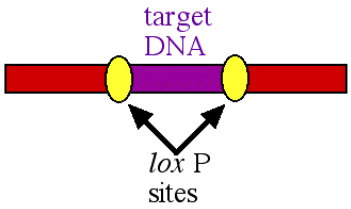

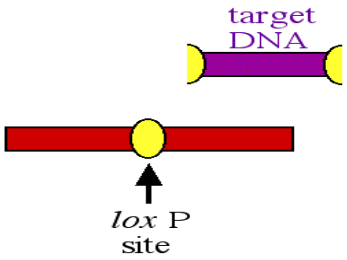

Figure 8A[130]. **Figure 8B**[130]**.**

Figure 8: Cre recombinase action mechanism

The outcome of a Cre-lox recombination is determined by the orientation and location of flanking loxP sites[131]. If the loxP sites are oriented in opposite directions, Cre recombinase mediates the inversion of the floxed segment (Figure 9A). If the loxP sites are located on different chromosomes (trans arrangement), Cre recombinase mediates a chromosomal translocation (Figure 9B). If the loxP sites are oriented in the same direction on a chromosome segment (cis arrangement), Cre recombinase mediates a deletion of the floxed segment (Figure 9C)[131].

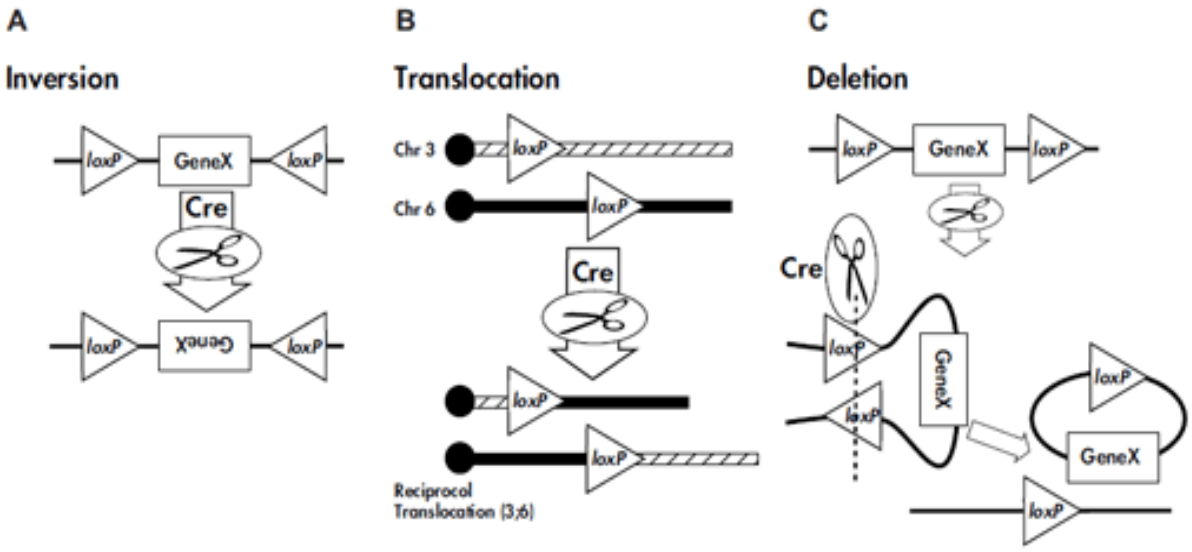

Figure 9: loxP orientation[131].

The directed introduction of null mutations into defined genes has proven invaluable in elucidating gene function in experimental mice[132]. However, targeted null mutations in a gene of interest can lead to embryonic lethality in mice, thus obscuring the particular role of that gene in a target tissue or in the adult[132]. Site-specific recombination strategies circumvent the problem of embryonic lethality by directing gene ablation in a spatially and temporally controlled manner[132]. As the Cre recombinase of phage P1 catalyzes efficient excisive recombination in mammalian cells[133], it has become a useful tool for generating a conditional knockout[134].

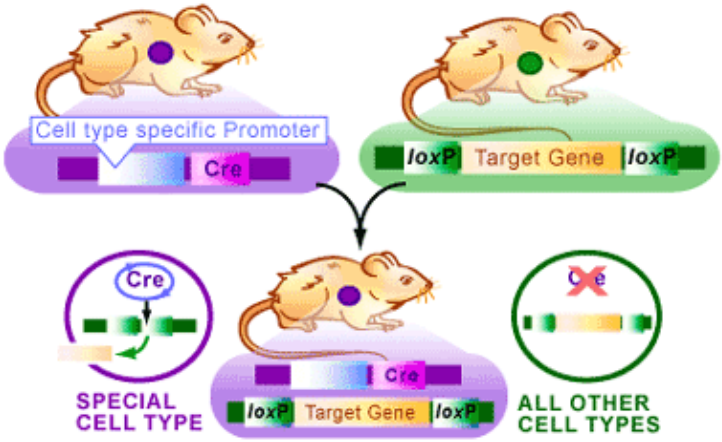

Figure 10: Cell type specific Cre recombination

Figure 10[117]**.** *The cell type specific promoter leads to Cre expression only in specific cells (violet). When such a cre transgenic is bred with a mouse containing the target gene flanked by loxP sites (green), their progeny will have the target gene deleted only in those cells where Cre expresses (violet).*

Conditional gene deletion allows assessment of a gene's function in a target tissue without disturbing expression of that gene in non-target tissues[132]. Two components are required: floxed mice created by homologous recombination (i.e., mice carrying two loxP sites surrounding the gene of interest), and a *cre* transgenic mouse that expresses Cre under the control of a promoter with the desired spatial and temporal pattern of expression. The exact placement of *lox* sites in the target gene depends both on the type of deletion event desired and on constraints imposed by the structure of the target gene[132]. Floxed mice are then crossed to mice expressing Cre recombinase leading to permanent inactivation of the gene based on the pattern of Cre expression that can be controlled with cell type specific promoters[3] like CNPase (Figure 10). Therefore, if the *cre* gene is bound to a promoter that allows Cre production only in neuronal cells, the target gene will be deleted in those cells alone[117]. This method allows researchers

to isolate the effects of genes in specific tissues, thereby providing very specific analysis of gene function[117].

Regulation can also be programmed in specific temporal patterns if the Cre expression is driven by the Tet-regulatory system. In case of a Tet-On system, Cre would be expressed, and consequently the gene deletion would occur, only in the presence of doxycycline.

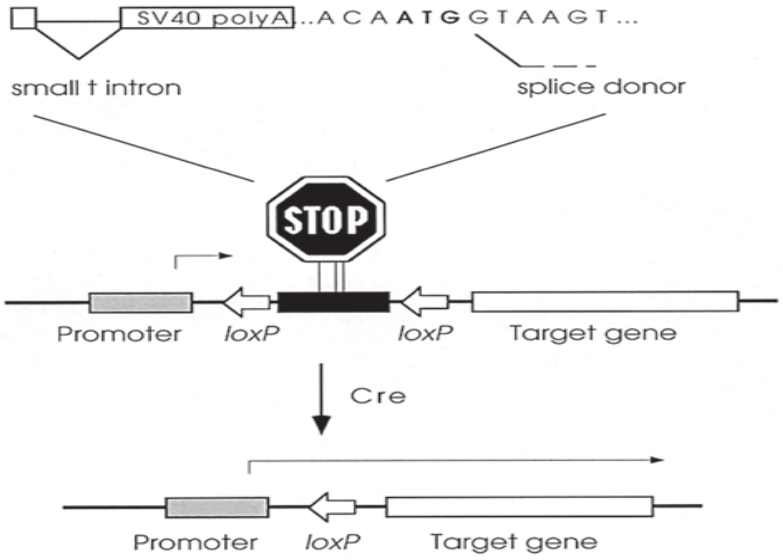

Figure 11: Cre recombinase for the targeted activation of genes[132].

In addition, Cre mediated excision has proven to be a very useful tool for targeted activation of genes in transgenic mice. A "STOP" cassette flanked by two directly repeated *loxP* sites (a lox^2 STOP cassette) is placed between the promoter and the gene to be activated (Figure 11) [135]. STOP is designed to block gene expression and consists of a stuffer region (from the yeast *HIS3* gene), the SV40 polyadenylation region, and errant optimized ATG translational start and splice donor signals[132]. Cre-mediated excision removes STOP thus permitting target-gene expression under the control of the adjacent promoter[132]. Two animals are required: one expressing Cre with the desired

spatial and temporal pattern and the other carrying a *lox*^{2} STOP-equipped transgene[132]. Mating of these two animals results in the activation of the target gene in those cells that express both Cre recombinase and are capable of expressing the target gene, as determined by the specificity of the promoter used in the *lox* target strain[132].

II) MATERIALS & METHODS

Tissue culture: Hek-293T cells were cultured in Dulbecco's Modified Eagle's Medium (DMEM) purchased from Mediatech, Inc. This medium is augmented with 4.5 g/L of glucose, L-glutamine and sodium pyruvate. The cells were seeded in a 6 well plate such that they reach 70% confluence in 24 hours. 24 hours from seeding, 5 of the wells were transfected with the CNPase-rtTA and P_{tight}-gene of interest using Lipofectamine™ 2000 (Invitrogen Corporation) as per the supplier's protocol. Opti-MEM reduced serum media, purchased from Invitrogen Corporation, was used as the cell transfection medium. 6 hours after transfection the reduced serum medium was replaced with the regular high-glucose DMEM.

24 hours from transfection, the cells were treated with doxycycline HCL purchased from Research Products International Corp . Doxycycline was added to obtain the following concentrations: 0.01 μg/ml, 0.05 μg/ml, 0.1 μg/ml, 0.5 μg/ml. One of the wells containing transgene transfected cells was left untreated, which served as a negative control.

48 hours after drug treatment, the cells were imaged under the fluorescent microscope to view GFP expression.

Immunoblot analysis: 48 hours after drug treatment the cells were harvested and lysed in modified radioimmune precipitation buffer (mRIPA)[136], having defined buffer composition, and 1X Complete Protease inhibitors (Roche diagnostics). After brief sonication, the cell debris was sedimented at 10,000g for 10 minutes. Protein quantification of the total cell lysates was carried out using the Bio-Rad protein assay kit. Proteins were separated by SDS-PAGE and transferred onto nitrocellulose for immunoblot analyses. Immunoblots were quantified by densitometry with the aid of the ImageJ software and the transgene expression levels were normalized to β-actin.

II) RESULTS

1) CNPase promoter

1.1. CNPase-rtTA transgene construction: The CNPase promoter sequence was obtained based on the following figure (Refer Figure 5 for explanation):

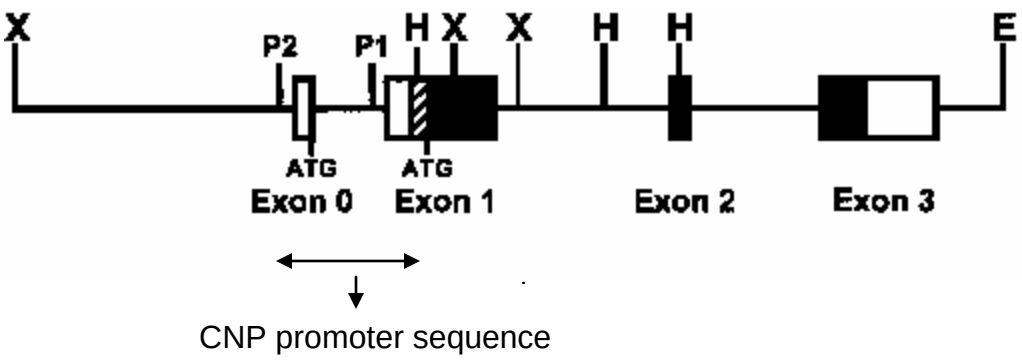

Figure 12: CNP promoter

The sequence between P2 (upstream of exon 0) and the HindIII site (in the non-coding sequence of exon 1) was obtained from the database (contig sequence 89518948-89525978 on chromosome 10). It contains both CNPase1 and CNPase2 promoter core elements. P1 and P2 indicate the two TATA-box sequences of CNPase1 and CNPase2 promoters, respectively[53]. The rtTA-Advanced sequence was taken from the pTet-On-Advanced vector (Figure 3c.) sequence (Clontech)[21].

EcoRI P2

GTAATGAGATCTGATGCCCTCTTCTGGTGTGAATTCGTCTGAAGACAGCTACAGTGTACTAATATATAATA
AATAAATAAGTCTTTAAAAAAAAAAGTTCGTCTCTCTCCTGGTAAAGTCTCTAATCTAAGCACTTGGGAGG
CAGAGGAGGCAGATCTCTCTATACCAGGCCAGCCTGATTTACAAAGTGAGTTCCAGGACGGCCAAGGCTAC
ATAGTGAGTCCCTGTCTCACAGGAGGGAAAAAGTTAATCTTCAACTTTTAAGTAACAAAGAGGTGGCGGAC
TCTTCTGGCATTGAGAGTCCAGGTGTGTTTTTGCTTTCTGCCAAGGCTCAGACAGCTGCTTCCTGGCACCC
AGGTTTCGATTCCCCGGGAGCGCGTGCGCAGAGGCTCGGGCTGACCCCGCCCCGTCCGCGCGCCCCGCCCC
CGGGCTATGAAAGGAGCCCTGCGTGGGGTCCTGACACCCCGAGACGCCCCGTGTCCCTCGCGCAGGCGGGC
GGCCCCGGAGACATAGTGCCCGCAAAGGCGGTGACGGCGGTGCGCCCACTCATCATGGTGAGCGCAGCGCA

CNPase promoter {Exon0}

CGCGTGGGGGGCGGGGCGGGAGAGATGCTAACGGAAAGCGAAAGTCTTGAGGATGCGTGAGCAGAAGTAGC
TTGCAAGTGAGGACACCAGGTTCCGAAGTTGAAGTCCAATCTCTGGGTCCTCCGAGGTAGCCCGAAGGCGG
GGAAGTTAGGGGGATTCTCAGTGTCTTTGGAGAAGGAAATATGGTAGCAAGAAAGAGAAAGTCGATGCGCC
CTGGAGACAACAGCTGGCAAATGGGCCTGTGCTCGGGGTAGCACCAGAGAGTCCAGGGCTGATGTCGAGCC
CTCGCGGGAGTGGGTTCCGAACCGCTTCCTGCTCAAGGCTATAGCGAAGCTGTAAGCCAGCTAAATTCTTA
AGGGTGCACACCAAAGGCGGAAGCCAGTGTAGATGACAATTGAAACCGCTATTCCTTGTTGCTTTTGTCAG
AGAGGTGCTGCTAACACACAGCCAAGTAGGGGGCAAAAATCCCTGAATACAGGTGCCCTGTGCTCCCTAGT
CCTACAGATTGGGGGAGGGGGTACAGCGAGAGCAGAGGAGGAGGTGGATGTGAATGAGGCCCTTTGTCCAG
TGCCCTCCTGCCCTGCCCCCCACTAGCCCTCTGTGGGACCATTGTCCCCCCACACCCAGACAAGAGAGTAT
TATCTGTTGGTGCCATTGTTGGGTGGAGGGAGGCGGTCTTTGGGTCACCCTCCTCTGCCCTCACCCTCCTC
TGCACACTCAGAAAGCCAGGGCAGCTGTGGCTTTGCCCAAACATAGAGCCTCAGGCTTCCACACAGGACAT
CCTTAAGAGGTGCCAAGAATATATAAGTTAGGGCTGACTGGGAGCAGCAGGCACTTGCTGCCCTTGCATGC

P1

CCTGCCACCAGGGTGTTCTCTCTGAGGGGTAGCTGAAAGCCGGGAGAGTAAGAGGTTTGATAGCTTCAGTG
AGGGTCCTTCTACTCATACAACCCTGCTGTTGAAGATACGGAAGGACCAGCTGGGAGGAAGAAAAGCTACC
ATTCCCTGCCGGGAGCTGGGAAAAGCGCCCACCATTCAAGGGTGCTTCAAGTTAGGCTCGGGGATTCCTGA

ACTGACATCCGGTCCCCCTCTGGGAGAACTAGGCCAAAGACAAGGGTTTGGTGCTTGTGGGCTGGCTTTGA
GGAGCCCGGGCTAACATCTCCTCCTCCCTTCTCACATAGAGCACAAGCTTGCCACCATGG
{Exon1 begins}
ctagactggaca agagcaaagt cataaacggc gctctggaat tactcaatgg agtcggtatc
gaaggcctga cgacaaggaa actcgctcaa aagctgggag ttgagcagcc
taccctgtac
tggcacgtga agaacaagcg ggccctgctc gatgccctgc caatcgagat
gctggacagg
catcataccc acttctgccc cctggaaggc gagtcatggc aagactttct
gcggaacaac
gccaagtcat tccgctgtgc tctcctctca catcgcgacg gggctaaagt
gcatctcggc rtTA-advanced (Pink)
acccgcccaa cagagaaaca gtacgaaacc ctggaaaatc agctcgcgtt
cctgtgtcag
caaggcttct ccctggagaa cgcactgtac gctctgtccg ccgtgggcca
ctttacactg
ggctgcgtat tggaggaaca ggagcatcaa gtagcaaaag aggaaagaga
gacacctacc
accgattcta tgcccccact tctgagacaa gcaattgagc tgttcgaccg
gcagggagcc
gaacctgcct tccttttcgg cctggaacta atcatatgtg gcctggagaa
acagctaaag
tgcgaaagcg gcgggccggc cgacgccctt gacgattttg acttagacat
gctcccagcc
gatgcccttg acgactttga ccttgatatg ctgcctgctg acgctcttga
cgattttgac
cttgacatgc tccccgggta actaagata cattgatgag

tttggacaaa ccacaactag aatgcagtga aaaaaatgct ttatttgtga aatttgtgat

gctattgctt tatttgtaac cattataagc tgcaataaac aagttaacaa caacaattgc

attcatttta tgtttcaggt tcaggggggag SV40polyA gtgtgggagg ttttttaaag

caagtaaaac ctctacaaat gtggtatggc tgattatgat cctgcaagcc tcgtcgtctg

gccggaccac gctatctgtg caaggtcccc ggacgcgcgc tccatgagca gagcgcccgc

cgccgaggca agactcgggc ggcgccctgc ccgtcccacc aggtcaacag gcggtaaccg

gcctcttcat cgggaatgcg cgcgaccttc agcatcgccg gcatgtcccc tggcggacgg

gaagtatAAGCTT(HindIII)

Figure 13: Sequence for CNPase promoter-rtTA advanced-polyA signal

The above sequence was given to GenScript for synthesis. The company synthesized the sequence and cloned it into pUC57 (2.7kb) using EcoRI and SalI**:** *Gene Length = 2.96kb; GenScript Clone ID = C10929*.

On receiving the product, a confirmation digest was carried out. The plasmid was cut with SalI alone, EcoRI alone, and double digested with SalI and EcoRI. The digested products were run on a 1% agarose gel along with a 1kb plus ladder (Invitrogen) (Figure 14).

Component	**SalI**	**EcoRI**	**SalI&EcoRI**
Buffer3(NEB)	2µl	2µl	2µl
BSA	0.5 µl	0.5 µl	0.5 µl
DNA	1 µg	1 µg	1 µg
EcoRI	-	0.5 µl	0.5 µl
SalI	0.5 µl	-	0.5 µl
Water	16 µl	16 µl	15.5 µl

37°C for 2 hours

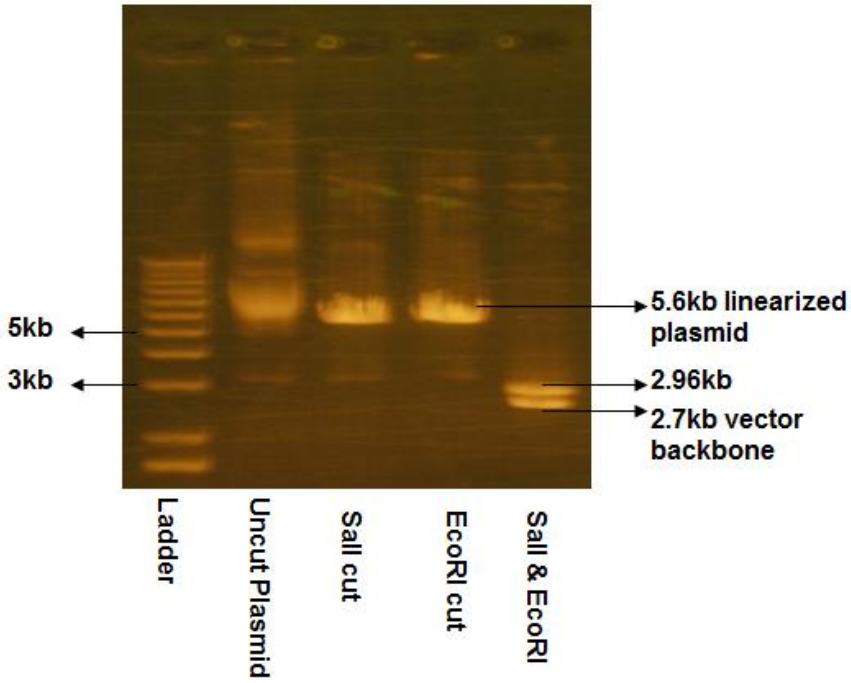

Double digestion with EcoRI and SalI yielded the expected 2.96kb CNP-rtTA-polyA band and the 2.7kb vector backbone.

Figure 14: CNPase-rtTA pUC57 confirmation digest

2) DN-ErbB4

2.1) pTRE-Tight-Bi-AcGFP1-DnErbB4 construct development

The pTRE-Tight-Bi-AcGFP1-DN-ErbB4 construct was generated in the lab prior to the commencement of this project. A construct containing DN-ErbB4 cloned into pcDNA3.1 was digested with ApaI, blunt ended, and subsequently digested with NotI to excise out the DN-ErbB4 from pcDNA3.1. The pTRE-Tight-Bi-AcGFP1 vector[21] provided by Clontech was digested with NotI and EcoRV. The 5' NotI ends and the 3' blunt ends of the DN-ErbB4 fragment and the pTRE-Tight-Bi-AcGFP1 vector were cloned together.

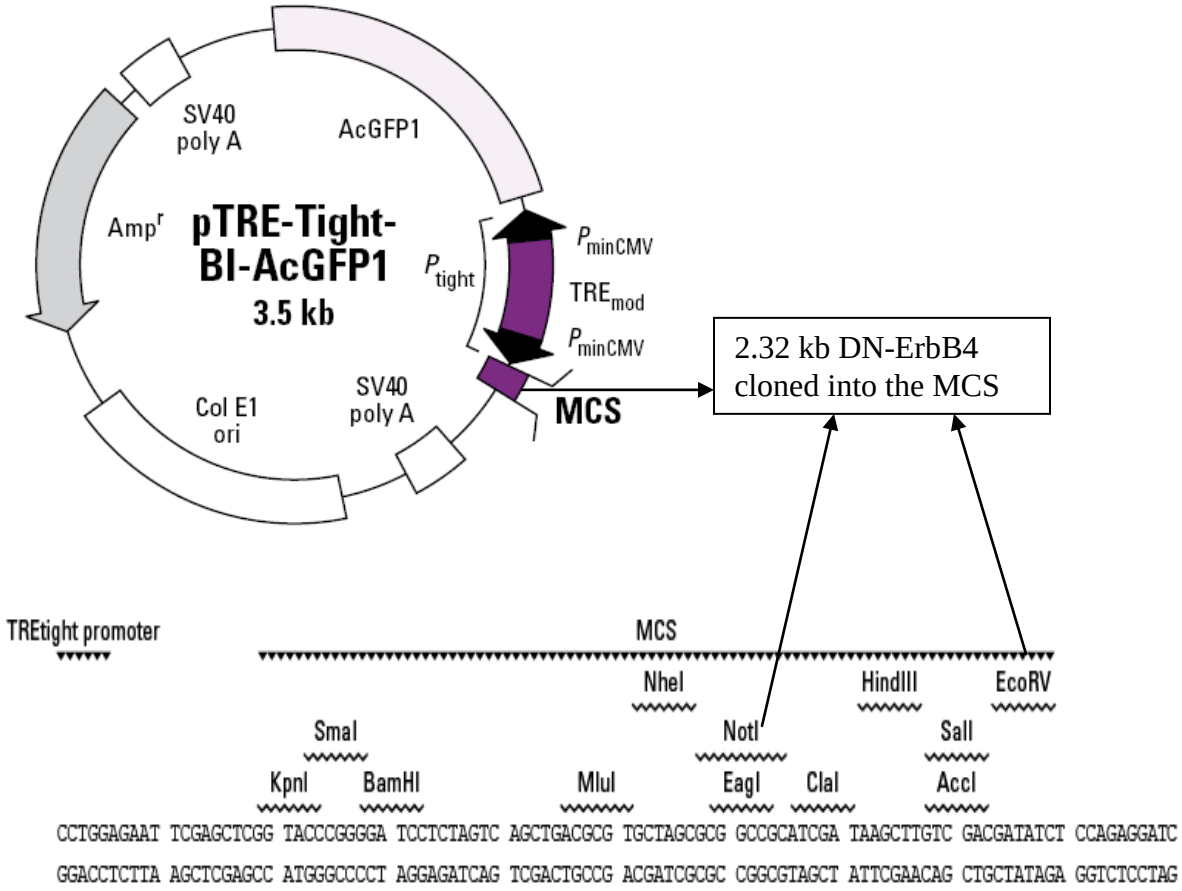

Figure 15: pTRE-Tight-Bi-AcGFP1-DN-ErbB4 cloning

The cloned product was sequenced using the primer, 3'-dnErbB4 in TreTight GFP.

Sequencing primer: **5'- CCA GAG GCA GGT AAC GAA AC - 3'**

2.2) Tet-On regulated expression of DN-ErbB4 in Hek293T cells.

Day1: Hek293T cells were seeded in a 6-well plate.

Day2: 24 hours from seeding, the cells reached 70% confluence. At this stage they were transiently transfected with CNPase-rtTA and DN-ErbB4 in a 1:1 ratio.

Day3: The cells were treated with various concentrations of doxycycline:

0, .01µg/ml, .05 µg/ml, 0.1 µg/ml, 0.5 µg/ml.

Day5: Cells were harvested and DN-ErbB4 expression was analyzed by immunoblotting.

2.2a) GFP expression

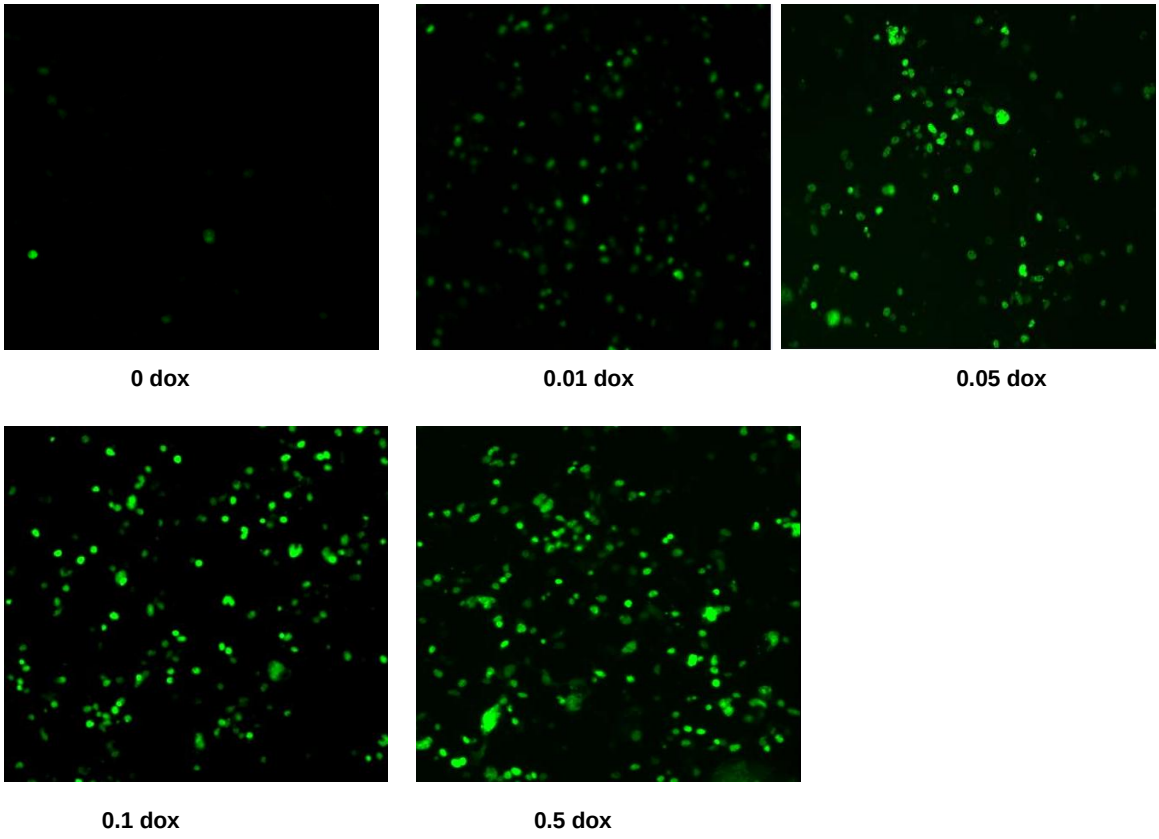

Figure 16: GFP expression by the DN-ErbB4 construct

Figure 16. 48 hours after drug treatment the GFP expression was observed at 40X magnification under an epifluorescence microscope. Shown above are the fluorescing cells at different doses of doxycycline (drug concentrations are in μg/ml). Cells that were not treated with doxycycline had minimal green fluorescence.

2.2b) DN-ErbB4 expression

Immunoblot analysis was carried out to determine the DN-ErbB4 expression level at different concentrations of doxycycline. On day 5 of the experiment the transfected and drug treated Hek293T cells were harvested and their lysates were prepared for immunoblot analysis. Samples were resolved by SDS-PAGE using a 7.5% acrylamide gel. Western blot was performed using a monoclonal antibody against the flag epitope present in the DN-ErbB4 construct. The monoclonal ANTI-FLAG antibody produced in mouse was purchased from Sigma Aldrich. Overnight incubation of the blot with the antibody (1:2000) at 4 degree Celsius followed by chemiluminescent detection yielded the following result.

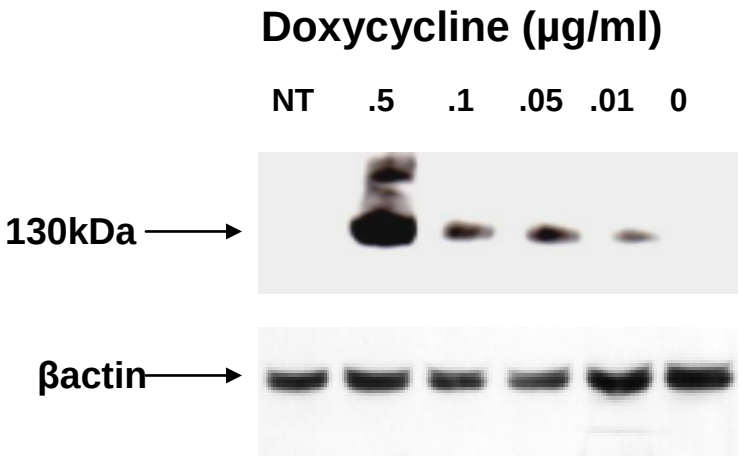

Figure 17A

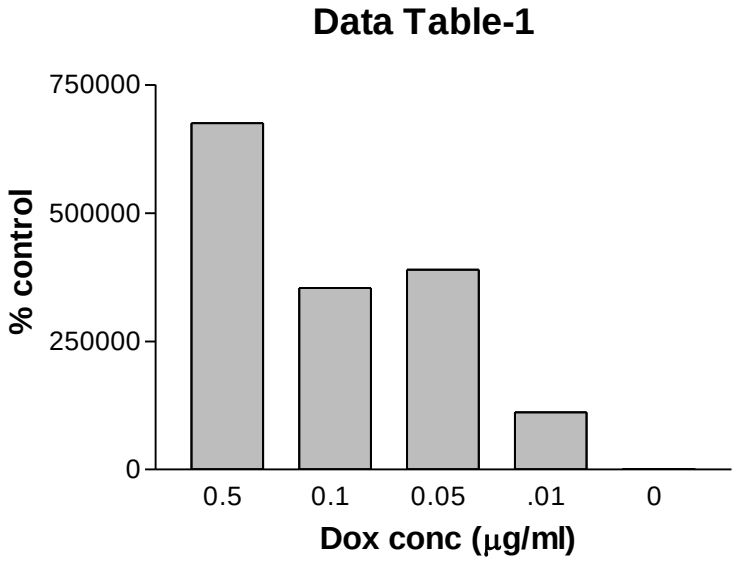

Figure 17b.

Figure 17: Dn-ErbB4 immunoblot analysis

Figure 17a shows the immunoblot analysis demonstrating an increase in the DN-ErbB4 expression level with increasing concentrations of Dox. The cells that were not treated with Dox, did not express DN-ErbB4. The untreated cells served as the control for transfected cells, while, the non-transfected cells were a negative control and indicate the specificity of the antibody for detecting DN-ErbB4 (NT= non-transfected).

Figure 17b shows the immunoblot quantitation of DN-ErbB4. Levels of DN-ErbB4 expression were normalized to β-actin and expressed as percent control. The blot-area of the control group was assigned an arbitrary value of 1 since this group showed undetectable levels of DN-ErbB4.

Summary: The immunoblot quantitation showed that DN-ErbB4 induction in the cells treated with 0.5μg/ml Dox displayed 6,753 fold induction of DN-ErbB4 when compared to the untreated cells. In the absence of Dox, basal expression was undetectable. Thus, the

CNPase-rtTA; TRE-DN-ErbB4 bi-transgenic system works in a tight and highly inducible manner in Hek293T cells.

2.3) Pronuclear microinjection & Analysis of transgenics

2.3a) Pronuclear microinjection

CNPase-rtTA digestion: For pronuclear microinjection, CNPase-rtTA was excised out of the pUC57 vector backbone.

Since CNPase-rtTA was cloned into pUC57 using EcoRI and SalI, these enzymes were used to excise out the insert from the vector (Refer Figure 14).

As seen in figure 14, the 2.96 kb CNPase-rtTA insert is very close to the 2.7 kb vector backbone band, so it was necessary to further fragment the vector backbone band. Therefore, apart from EcoRI and SalI, BglI and ScaI were used to digest the CNPase-rtTA-pUC57 plasmid. The reaction was carried out in buffer D at 37°C overnight. Since the BglI and ScaI sites are present in the pUC57 vector backbone, the previously mentioned digestion was able to fragment the 2.7 kb vector backbone band to yield the following result:

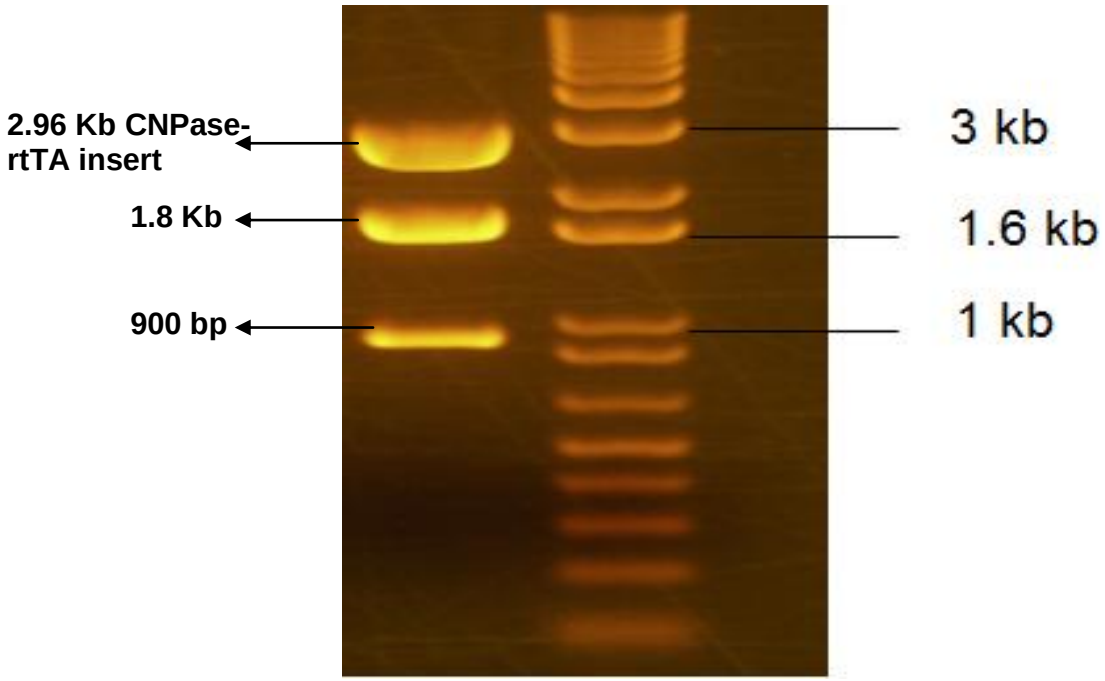

Figure 18: CNPase-rtTA digestion for pronuclear microinjection

The 2.9 kb CNPase-rtTA insert was gel purified and given to the Transgenic and Knockout Mouse Laboratory at the University of Kansas (TKMKU) for pronuclear microinjection.

TREtight-DN-ErbB4 digestion: TREtight-DN-ErbB4 was excised out of the pTRE-Tight-AcGFP1 vector backbone for pronuclear microinjection.

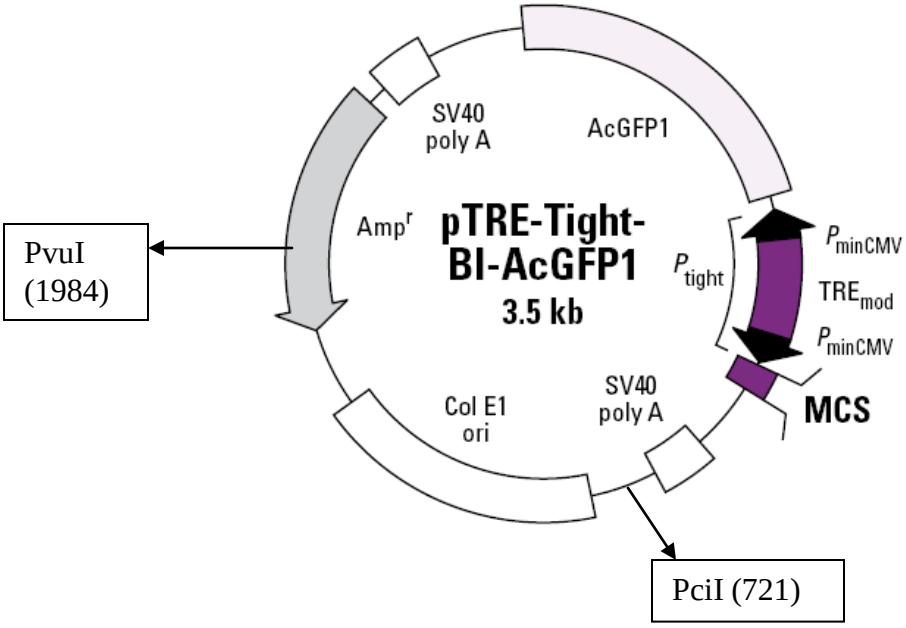

Figure 19: PvuI and PciI sites on the pTRE-Tight-AcGFP1 vector

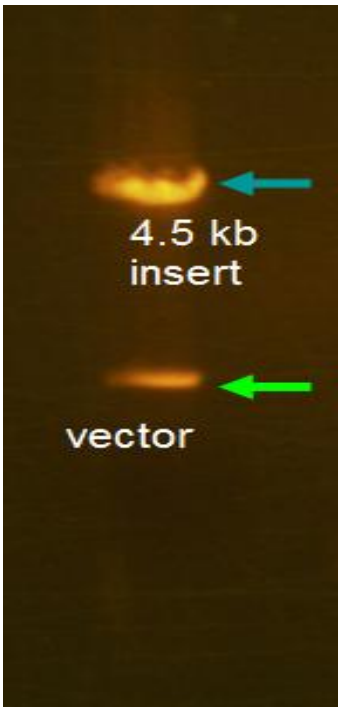

Figure 19 shows the PvuI and PciI sites present in the pTRE-Tight-AcGFP1 vector. The pTRE-Tight-AcGFP1-DN-ErbB4 plasmid was digested with these two enzymes to yield the following result (Figure 20)

Figure 20: pTRE-Tight-AcGFP1-DN-ErbB4 plasmid digestion for pronuclear microinjection

As shown in figure 20, the 4.5 kb band includes the DN-ErbB4 insert, wherein the 1.2 kb band is the vector backbone sequence between the PvuI and PciI sites. The 4.5 kb band was gel purified and given to TMKU for pronuclear microinjection.

Once the transgenic mice are born after the pronuclear microinjection of CNPase-rtTA and TREtight-DN-ErbB4, they need to be tested for the presence of the transgenes. In order to do so, primers were designed against the two transgenes and their respective PCR conditions were standardized.

2.3b) Standardizing the PCR conditions for CNPase-rtTA

200 ng of the CNPase-rtTA plasmid DNA was used for PCR amplification. Reaction conditions were as follows:

Components	**Volume**
10X Thermopol buffer (NEB)	2 µl
10mM dNTP	1 µl
CNPase-rtTA plasmid	200ng
20µM 5' CNPase promoter primer	0.5 µl
20µM 3' rtTA advanced primer	0.5 µl
Deep vent taq polymerase	0.2 µl
Water	14.8 µl

PCR program:

95°C - 5 minutes

95°C - 30 seconds

58°C - 30 seconds

72°C - 30 seconds

34 cycles repeat

72°C – 5 minutes

4°C - hold

5' CNPase promoter primer sequence: 5'- TGA AAG CCG GGA GAG TAA GA- 3'

3' rtTA Advanced primer sequence: 5'- CTT GTT CTT CAC GTG CCA GT- 3'

A temperature gradient was set up in order to determine the optimum primer annealing temperature. The amplified products were run on a 1% agarose gel to resolve the required 450 bp amplicon.

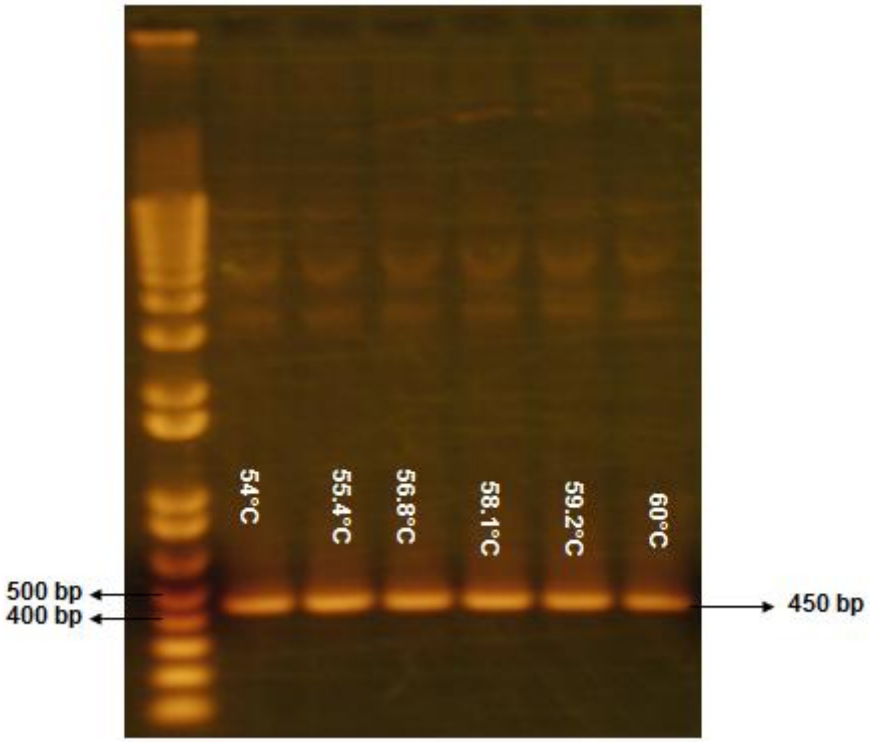

Figure 21: CNPase-rtTA PCR

Figure 21 shows the 450 bp CNPase-rtTA amplicon. The amplification worked at all the temperatures.

On pronuclear microinjection, the transgene randomly integrates into the genomic DNA of the mouse. PCR is used to amplify this integrated transgene in order to identify the transgenics in the litter. Since 200 ng of the CNPase-rtTA plasmid served as the template for the above mentioned PCR, it is important to ensure that these conditions are also optimum for the amplification of low amounts of the transgene construct (in picograms) diluted in genomic DNA.

Calculation of Copy Number Standards:

Assumption: The haploid content of a mammalian genome is $3x10^9$ bp

Since the transgenic founder mice are hemizygous, the mass of transgene to be diluted in 1 μg of genomic DNA in order to make 1 copy standard equals:

$$\text{Mass of transgene DNA} = \frac{\text{bp transgene DNA}}{3x10^9 \text{ bp genomic DNA}} \times 1\ \mu g \text{ genomic DNA}$$

CNPase-rtTA transgene length = 5660 bp

$$\text{Therefore, mass of transgene to make 1 copy} = \frac{5660 \times 1\mu g \text{ genomic DNA}}{3x10^9 \text{ bp genomic DNA}} = 1.88 \text{ picograms in 1 } \mu g \text{ genomic DNA}$$

0.1 copy = 0.0376 picograms of transgene diluted in 200 ng of genomic DNA

1 copy = 0.376 picograms of transgene diluted in 200 ng of genomic DNA

10 copy = 3.76 picograms of transgene diluted in 200 ng of genomic DNA

50 copy = 18.8 picograms of transgene diluted in 200 ng of genomic DNA

100 copy = 37.6 picograms of transgene diluted in 200 ng of genomic DNA

The transgene plasmid was diluted into the genomic DNA extracted from a mouse ear piece to yield the above mentioned copy numbers. The PCR conditions standardized for 200 ng of CNPase-rtTA plasmid DNA were used to amplify the dilutions, keeping the primer annealing temperature at 58°C. The PCR products were run on a 1% agarose gel along with a 1kb plus ladder.

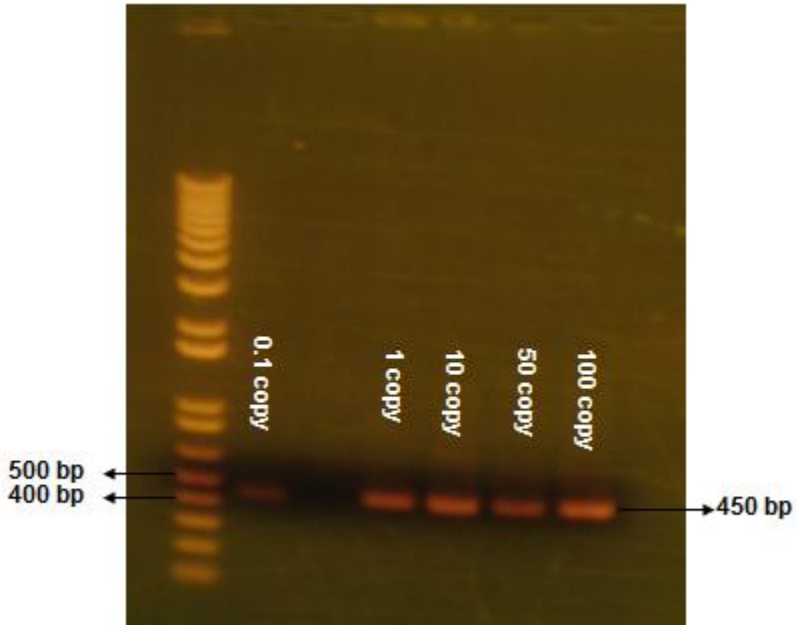

Figure 22: CNPase-rtTA vector dilution PCR

Figure 22 shows the amplification of different copy numbers of the transgene.

2.3c) Standardizing the PCR conditions for pTRE-Tight-Bi-AcGFP1-DN-ErbB4

200 ng of the pTRE-Tight-Bi-AcGFP1-DN-ErbB4 plasmid DNA was used for PCR amplification. Reactions were carried out at different concentrations of Mg^{2+} ion (2mM-7mM). The primer annealing temperature was kept constant at 58°C for all reactions. Reaction conditions were as follows:

Components	Volume
10X Ex Taq buffer (Mg^{2+} free; TaKaRa)	5 µl
10mM dNTP	4 µl
DN-ErbB4 containing plasmid	200ng
20µM 5' Tre-Tight GFP primer	0.5 µl
20µM 3' dn-ErbB4 in TreTight GFP primer	0.5 µl
Ex taq	0.25 µl
Magnesium ion	2mM-7mM final concentration
Water	Total volume made up to 50 µl

PCR program:

95°C - 5 minutes

95°C - 30 seconds

58°C - 30 seconds

72°C - 30 seconds

34 cycles repeat

72°C – 5 minutes

4°C - hold

5' Tre-Tight GFP primer sequence: 5'-AAG TCG TGC TGC TTC ATG TG-3'

3'dn-ErbB4 in TreTight GFP primer sequence: 5'-CCA GAG GCA GGTAACGAAAC -3'

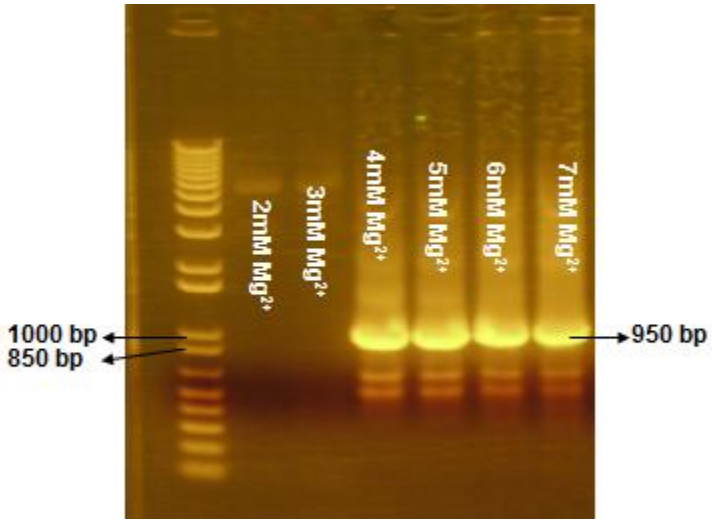

Figure 23: pTRE-Tight-Bi-AcGFP1-DN-ErbB4 PCR

The PCR products were run on a 1% agarose gel along with a 1kb plus DNA ladder. Figure 23 shows that 200 ng of the transgene plasmid amplified best when the reaction contained 4mM to 7mM Mg^{2+} ion.

The next step was to check if the above mentioned PCR conditions are optimal for amplifying the transgene plasmid diluted in genomic DNA.

Calculation of Copy Number Standards:

Assumption: The haploid content of a mouse mammalian genome is $3X10^9$ bp

Since the transgenic founder mice are hemizygous, the mass of transgene to be diluted in 1 µg of genomic DNA in order to make 1 copy standard equals:

$$\text{Mass of transgene DNA} = \frac{\text{bp transgene DNA}}{3x10^9 \text{ bp genomic DNA}} \times 1\ \mu g \text{ genomic DNA}$$

CNPase-rtTA transgene length = 5820 bp

$$\text{Therefore, mass of transgene to make 1 copy} = \frac{5820 \times 1\mu g \text{ genomic DNA}}{3x10^9 \text{ bp genomic DNA}} = 1.94 \text{ picograms in 1 } \mu g \text{ genomic DNA}$$

0.1 copy = 0.0388 picograms of transgene diluted in 200 ng of genomic DNA

1 copy = 0.388 picograms of transgene diluted in 200 ng of genomic DNA

10 copy = 3.88 picograms of transgene diluted in 200 ng of genomic DNA

50 copy = 19.4 picograms of transgene diluted in 200 ng of genomic DNA

100 copy = 38.8 picograms of transgene diluted in 200 ng of genomic DNA

The transgene plasmid was diluted into the genomic DNA extracted from a mouse ear piece to yield the above mentioned copy numbers. The PCR conditions standardized for 200 ng of pTRE-Tight-Bi-AcGFP1-DN-ErbB4 plasmid DNA were used to amplify the dilutions, keeping the primer annealing temperature at 58°C and using 5mM Mg^{2+} in the reaction mix. The PCR products were run on a 1% agarose gel along with a 1kb plus ladder.

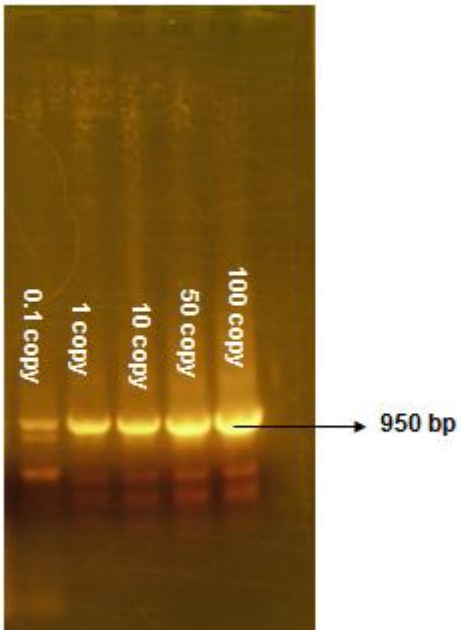

Figure 24: pTRE-Tight-Bi-AcGFP1-DN-ErbB4 vector dilution PCR

3) dnUbc9

3.1) pTRE-Tight-Bi-AcGFP1-dn-Ubc9 construct development

The plasmid, p3259 pCMV hUbc9 mt HA was purchased from Addgene, Inc. Figure 25 shows the map of this plasmid.

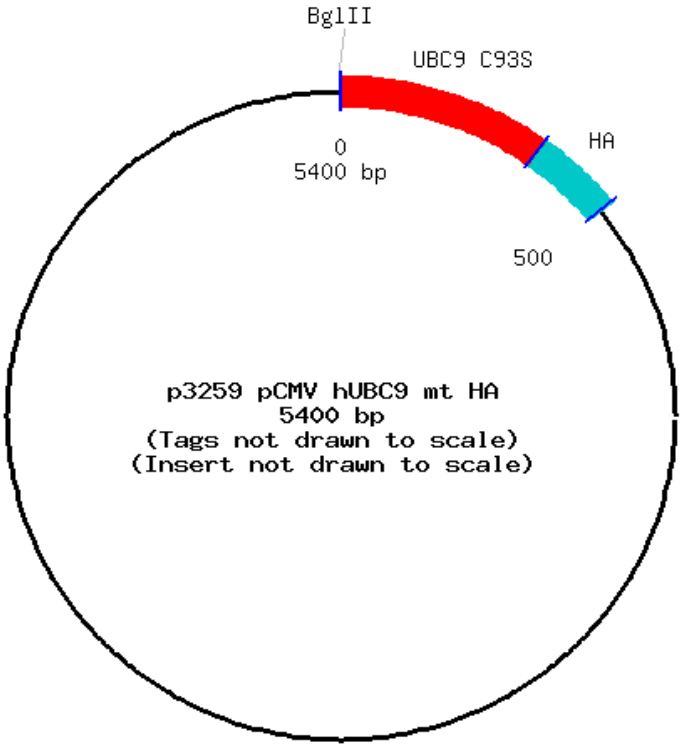

Figure 25: p3259 pCMV hUbc9 mt HA vector map

Plasmid details:

Vector backbone: pCMV4

Backbone size: 4900 bp

Gene/Insert: Ubc9 C93S-HA

Insert size: 500 bp

Species of gene: H.sapiens

Cloning site at 5’ end: BglII

3’ cloning site: BglII (site destroyed during cloning)

dn-Ubc9-HA description: A fragment containing the full coding region of dn-Ubc9 cDNA along with the influenza virus hemagglutinin 1 epitope (HA) sequence (YPYDVPDYA) at the 3′-end was produced with appropriate synthetic oligonucleotides using PCR, by Yasugi et al[85]. The fragment was then cloned into the pCMV4 vector at the BglII site[85].

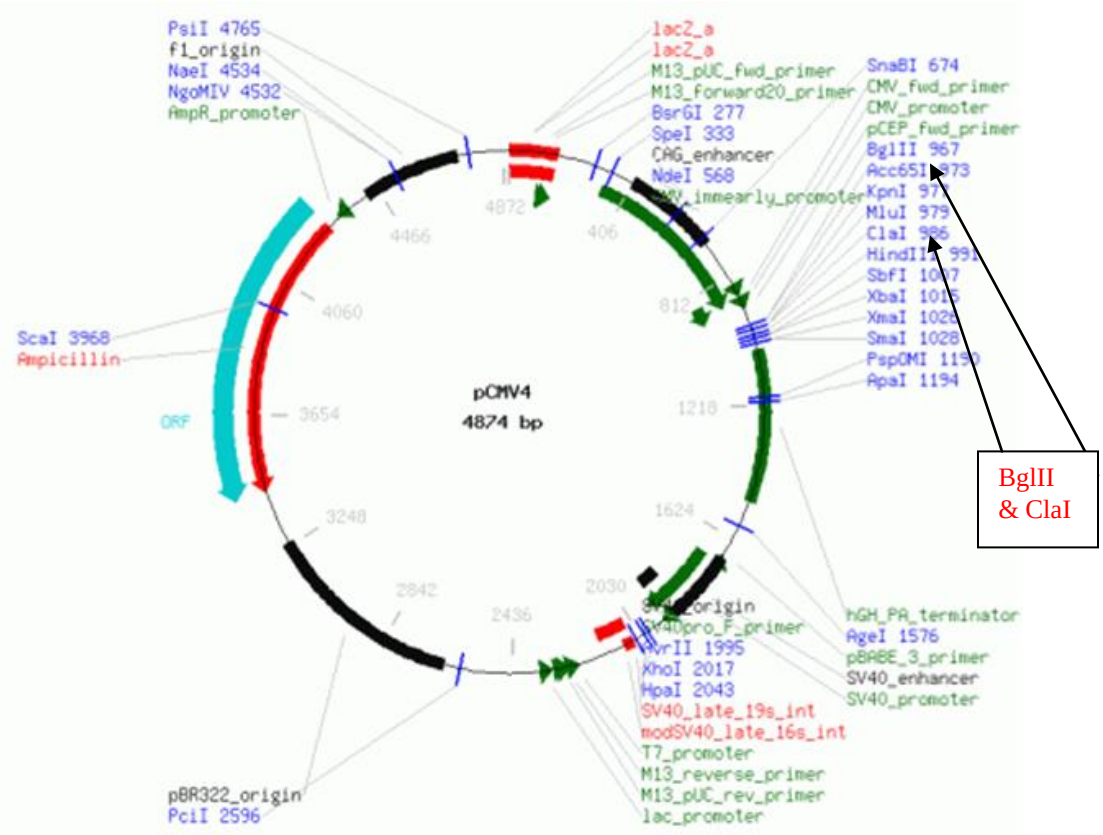

Figure 26: pCMV4 vector map

In order to develop the pTRE-Tight-Bi-AcGFP1-dnUbc9 construct, the 500 bp Ubc9mt-HA insert had to be excised from the pCMV4 vector backbone and cloned into the pTRE-Tight-Bi-AcGFP1 vector. Figure 26 shows the pCMV4 vector map. The Ubc9 mutant

was cloned into the BglII site of this vector, which is 20 bp upstream of a ClaI site. In order to excise the insert, the p3259 pCMV dnUbc9 HA plasmid was digested with BglII at the 5' end and ClaI at the 3' end. Digestion conditions were as follows:

Components	Amount
BufferD:	2 µl
BSA:	0.5 µl
DNA:	2 µg
BglII:	1 µl
ClaI:	1.5 µl
Water:	13.7 µl

→ Digested at 37°C for 2 hours.

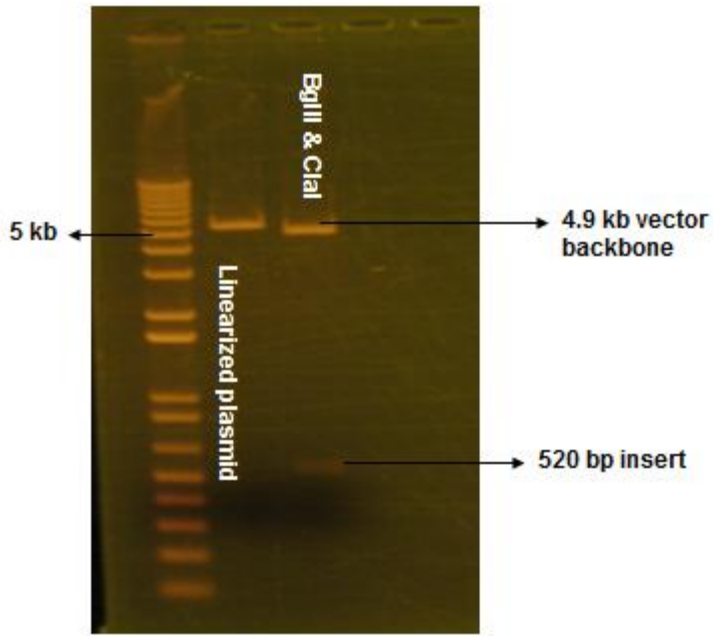

Figure 27: p3259 pCMV dnUbc9 HA plasmid digestion

Figure 27 shows the digestion of the p3259 pCMV dnUbc9 HA plasmid with BglII and ClaI. The first lane shows the 1kb plus DNA ladder, lane 2 shows the plasmid linearized with ClaI and lane 3 shows the plasmid double digested with BglII and ClaI to yield the 520 bp fragment.

Subsequently, the 520 bp insert was gel purified (with the Marligen gel purification kit) in order to be cloned into the pTRE-Tight-Bi-AcGFP1 vector. The vector was digested with BamHI at the 5' end and ClaI at the 3' end (Figure 27). The digestion conditions were as follows:

Components	Amount
NEB Buffer 4:	3µl
BSA:	1 µl
DNA:	1 µg
ClaI:	0.8 µl
BamHI:	0.5 µl
Water:	21.7 µl

→ Digested at 37°C for 2 hours.

The digested product was resolved on a 1% agarose gel and the band was gel purified using the Marligen gel purification kit. The 5' BglII end of the insert was subcloned into the 5' BamHI end of the vector, wherein, the 3' ClaI ends of both the vector and the insert were ligated using the quick ligation kit provided by NEB.

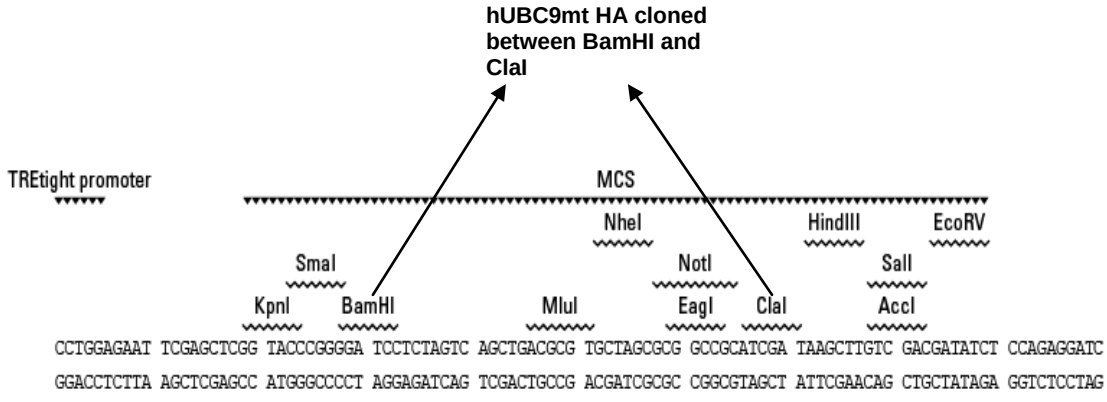

Figure 28: pTRE-Tight-Bi-AcGFP1-dnUbc9 cloning

Figure 28 *shows the hUBC9mt HA cloned between the BamHI and ClaI site present in the MCS of the pTRE-Tight-Bi-AcGFP1 vector.*

DH10B E.coli bacterial strain was transformed with the ligation product. Plasmid extracted from the transformed bacterial colonies were subjected to restriction digestion. Since the BamHI cloning site was destroyed during cloning, SmaI and ClaI were used to pop-out the dnUbc9 insert from the vector (Figure 29).

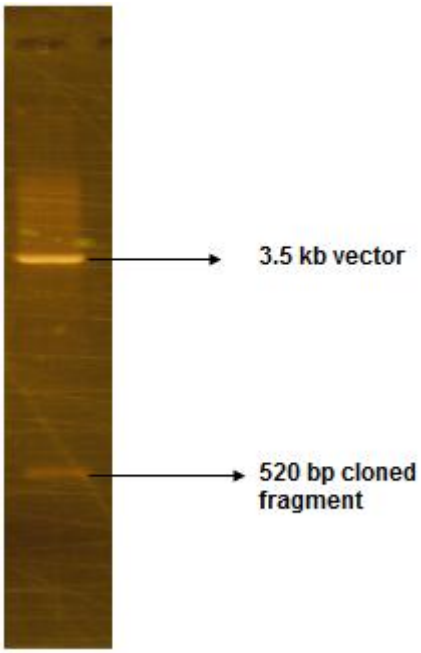

Figure 29: pTRE-Tight-Bi-AcGFP1-dnUbc9 digestion to confirm presence of insert

Figure 29 *shows the digest confirming the presence of dn-Ubc9 HA in the pTRE-Tight-Bi-AcGFP1 vector.*

The clone was sequenced using the primer; 5'TRE-Tight GFP

5' Sequencing primer: 5'- AAG TCG TGC TGC TTC ATG TG-3'

3.2) Tet-On regulated expression of dn-Ubc9 in Hek293T cells.

Day1: Hek293T cells were seeded in a 6-well plate.

Day2: 24 hours from seeding, the cells reached 70% confluence. At this stage they were transiently transfected with CNPase-rtTA and dnUbc9 in a 1:1 ratio.

Day3: The cells were treated with various concentrations of doxycycline:

0, .01µg/ml, .05 µg/ml, 0.1 µg/ml, 0.5 µg/ml.

Day5: Cells were harvested and dn-Ubc9 expression was analyzed by immunoblotting.

3.2a) GFP Expression

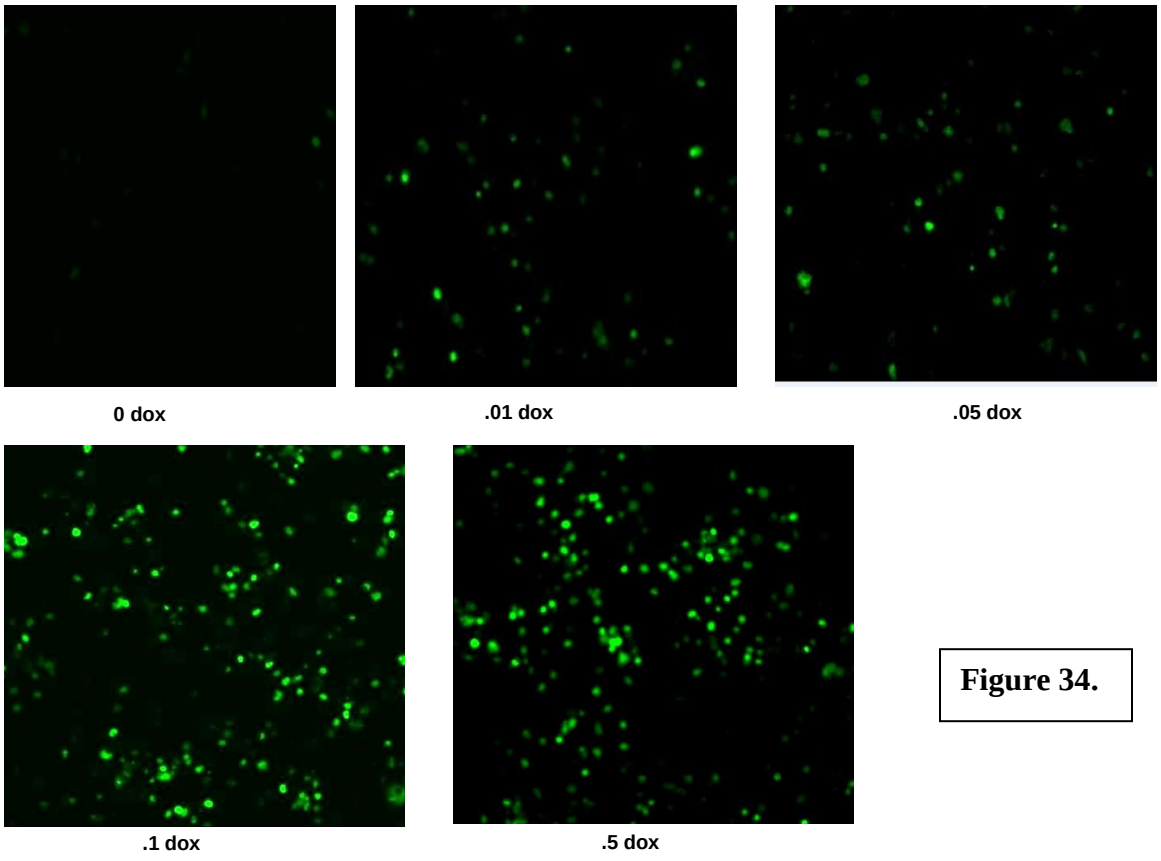

Figure 34.

Figure 30: GFP expression by the dnUbc9 construct

Figure 30. 48 hours after drug treatment the GFP expression was observed at 40X magnification under an epifluorescence microscope. Shown above are the fluorescing cells at different doses of doxycycline (drug concentrations are in μg/ml). Cells that were not treated with doxycycline had minimal green fluorescence.

3.2b) dnUbc9 expression

Immunoblot analysis was carried out to determine the dnUbc9 expression level at different concentrations of doxycycline. On day 5 of the experiment the transfected and drug treated Hek293T cells were harvested and their lysates were prepared for immunoblot analysis. Samples were resolved by SDS-PAGE using a 15% acrylamide gel. Western blot was performed using a monoclonal antibody against the HA tag present in the dnUbc9 construct. The mouse monoclonal antibody against HA was purchased from Covance. Overnight incubation of the blot with the antibody (1:1000) at 4°C followed by chemiluminescent detection yielded the following result.

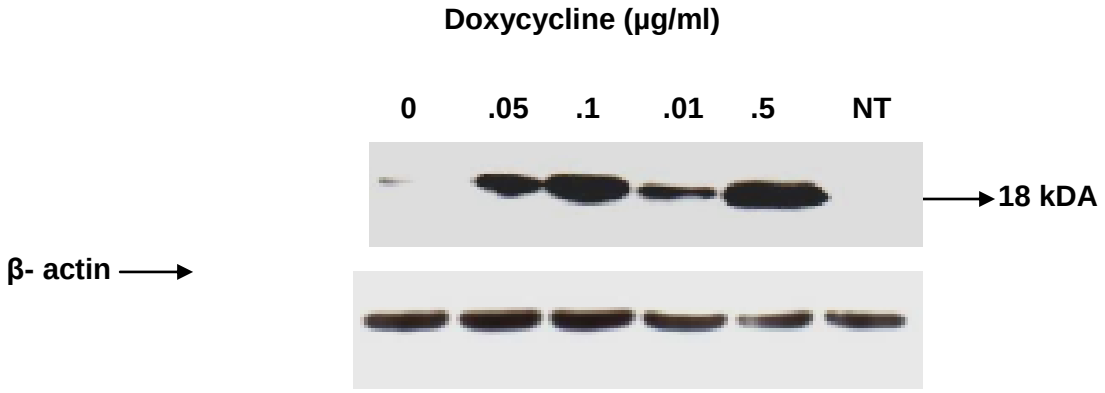

Figure 31a.

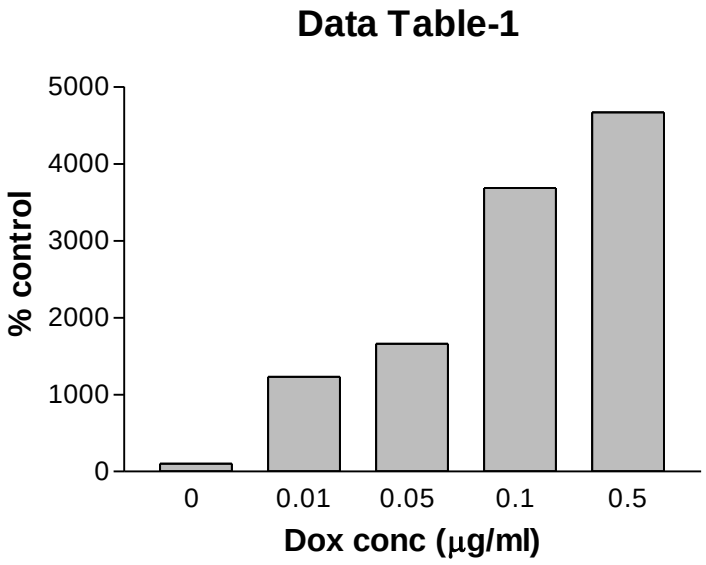

Figures 31b.

Figure 31: dnUbc9 immunoblot analysis

Figure 31a shows the immunoblot analysis demonstrating an increase in the dnUbc9 expression level with increasing concentrations of doxycycline. The cells that were not treated with doxycycline had minimal dnUbc9 expression. The untreated cells served as the control for transfected cells, while, the non-transfected cells were a negative control and indicate the specificity of the antibody for detecting dnUbc9. (NT= non-transfected)

Figure 31b shows the immunoblot quantitation of dnUbc9 by densitometry with the aid of the ImageJ software. Levels of dnUbc9 expression were normalized to β-actin and expressed as a percent of control.

Summary: The immunoblot quantitation showed that dnUbc9 induction in the cells treated with 0.5µg/ml Dox displayed a 47 fold induction of dnUbc9 when compared to the untreated cells. In the absence of Dox, basal expression was minimal. Thus, the CNPase-rtTA; TRE-dnUbc9 bi-transgenic system works in a tight and highly inducible manner in Hek293T cells.

3.3) Pronuclear microinjection & Analysis of transgenics

3.3a) Pronuclear microinjection

dnUbc9 was excised out of the pTRE-Tight-AcGFP1 vector backbone for pronuclear microinjection.

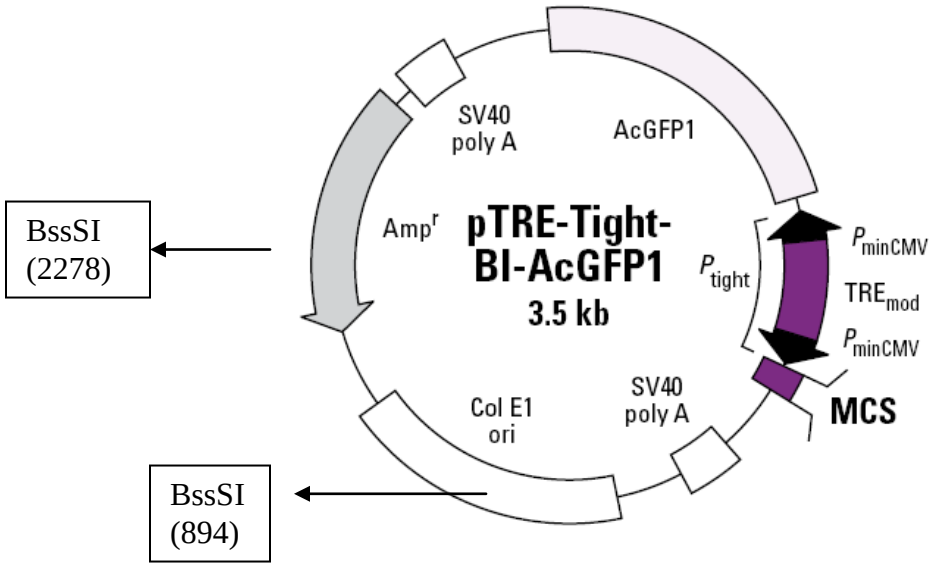

Figure 32: BssSI sites in the pTRE-Tight-AcGFP1 vector

Figure 32 shows the two BssSI sites present in the pTRE-Tight-AcGFP1 vector. The pTRE-Tight-AcGFP1-dnUbc9 plasmid was digested with this enzyme to yield the following result (Figure 33; Lane1)

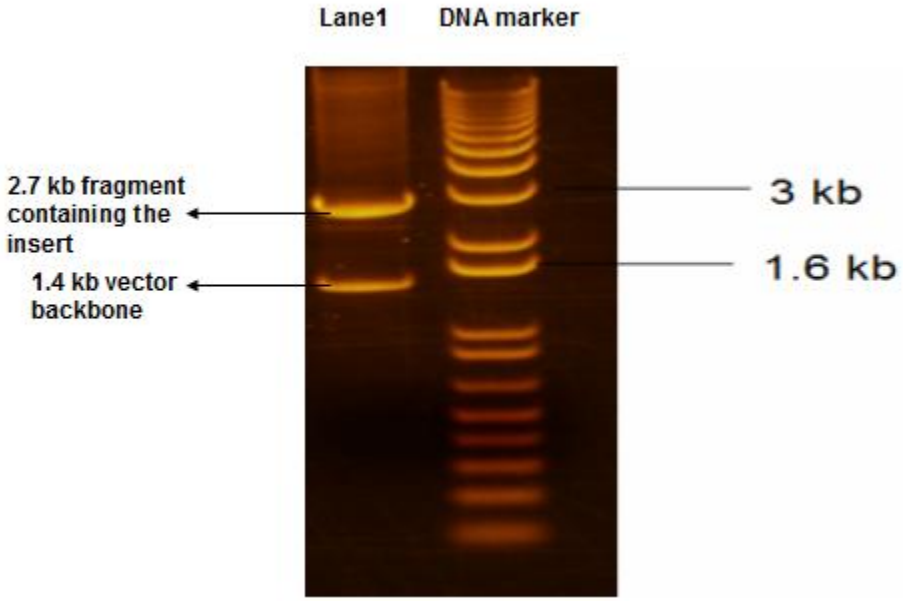

Figure 33: pTRE-Tight-AcGFP1-dnUbc9 plasmid digested for pronuclear microinjection

As shown in figure 33, the 2.7 kb band includes the dnUbc9 insert, wherein the 1.4 kb band is the vector backbone sequence between the BssSI sites. The 2.7 kb band was gel purified and given to TMKU for pronuclear microinjection.

Once the transgenic mice are born after the pronuclear microinjection of CNPase-rtTA and TREtight-dnUbc9, they need to be tested for the presence of the transgenes. In order to do so, primers were designed against the dnUbc9 containing transgene to standardize the PCR conditions.

3.3b) Standardizing the PCR conditions for pTRE-Tight-Bi-AcGFP1-Ubc9-DN

200 ng of the pTRE-Tight-Bi-AcGFP1-dnUbc9 plasmid DNA was used for PCR amplification. Reactions were carried out at different concentrations of Mg^{2+} ion (2mM-7mM). The primer annealing temperature was kept constant for all reactions (58°C). Reaction conditions were as follows:

Components	Volume
10X Ex Taq buffer (Mg^{2+} free; TaKaRa)	5 µl
10mM dNTP	4 µl
Ubc9-DN containing plasmid	200ng
20µM 5' Tre-Tight GFP primer	0.5 µl
20µM 3' Ubc9-DN in TreTight GFP primer	0.5 µl
Ex taq DNA polymerase	0.25 µl
Magnesium ion	2mM-7mM final concentration
Water	Total volume made up to 50 µl

PCR program:

95°C - 5 minutes

95°C - 30 seconds

58°C - 30 seconds

72°C - 30 seconds

34 cycles repeat

72°C – 5 minutes

4°C - hold

5' Tre-Tight GFP primer sequence: 5'-AAG TCG TGC TGC TTC ATG TG-3'

3'Ubc9-DN in TreTight GFP primer sequence: 5'-ATG AGG TTC ATC GTG CCA TC-3'

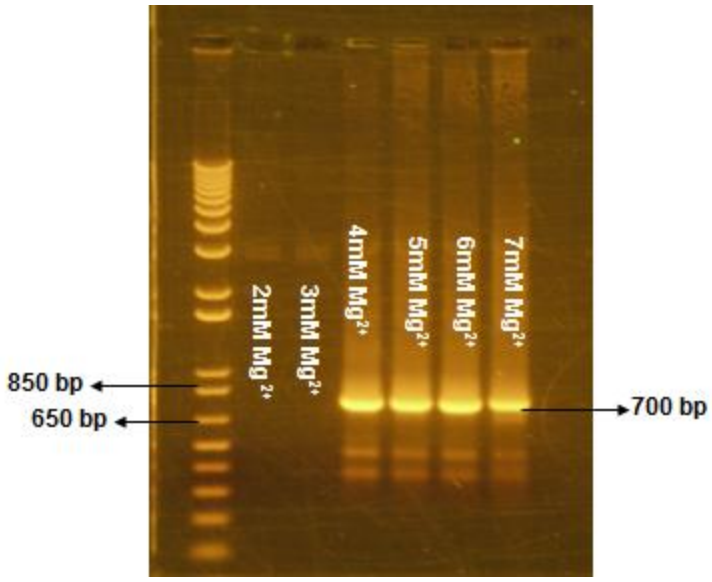

Figure 34: pTRE-Tight-AcGFP1-dnUbc9 PCR

The PCR products were run on a 1% agarose gel along with a 1kb plus DNA ladder. Figure 34 shows that the transgene plasmid amplified best when the reaction contained 4mM to 7mM Mg^{2+} ion.

The next step was to check if the above mentioned PCR conditions are optimal for amplifying the transgene plasmid diluted in genomic DNA.

Calculation of Copy Number Standards:

Assumption: The haploid content of a mouse mammalian genome is $3X10^9$ bp

Since the transgenic founder mice are hemizygous, the mass of transgene to be diluted in 1 µg of genomic DNA in order to make 1 copy standard equals:

$$\text{Mass of transgene DNA} = \frac{\text{bp transgene DNA}}{3x10^9 \text{ bp genomic DNA}} \times 1 \text{ µg genomic DNA}$$

Ubc9-DN containing plasmid's length = 4020 bp

$$\text{Therefore, mass of transgene to make 1 copy} = \frac{4020 \times 1\text{µg genomic DNA}}{3x10^9 \text{ bp genomic DNA}} = 1.34 \text{ picograms in 1 µg genomic DNA}$$

0.1 copy = 0.027 picograms of transgene diluted in 200 ng of genomic DNA

1 copy = 0.27 picograms of transgene diluted in 200 ng of genomic DNA

10 copy = 2.7 picograms of transgene diluted in 200 ng of genomic DNA

50 copy = 13.5 picograms of transgene diluted in 200 ng of genomic DNA

100 copy = 27.0 picograms of transgene diluted in 200 ng of genomic DNA

The transgene plasmid was diluted into the genomic DNA extracted from a mouse ear piece to yield the above mentioned copy numbers. The PCR conditions standardized for 200 ng of pTRE-Tight-Bi-AcGFP1-dnUbc9 plasmid DNA were used to amplify the dilutions, keeping the primer annealing temperature at 58°C and using 4mM Mg^{2+} in the reaction mix. The PCR products were run on a 1% agarose gel along with a 1kb plus ladder.

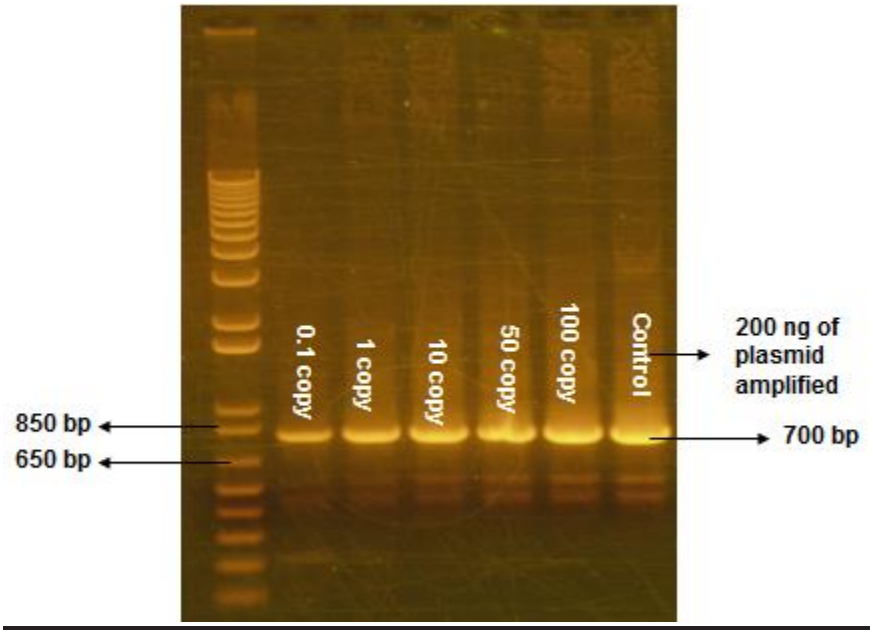

Figure 35: pTRE-Tight-AcGFP1-dnUbc9 vector dilution PCR

4) Cre

4.1) pTRE-Tight-Cre construct development

The plasmid, pBS595 tet-hCMV-EGFPcre was purchased from Addgene, Inc.

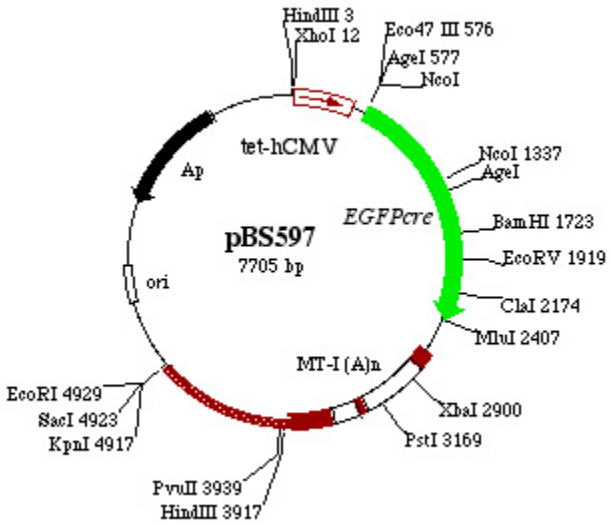

Figure 36: pBS597 vector map

Figure 36 shows the map of the pBS597 plasmid. pBS595 differs from pBS597 in having the GCSF A(n) instead of the MT-I A(n). pBS597 carries the EGFPcre fusion gene under the control of a synthetic promoter that can be regulated by a synthetic tet repressor/activator protein. In the presence of doxycycline expression is dramatically turned on to high levels. The GFP moiety of the fusion gene carries the S65T mutation for enhanced fluorescence and is codon-optimised for higher level expression.

pBS595 details:

Gene/Insert: EGFP-cre

Insert size: 1800 bp

Species of gene: bacteriophage P1

The pBS595 plasmid was linearized with XhoI, ClaI, and double digested with these enzymes using NEB buffer 4. The following was obtained:

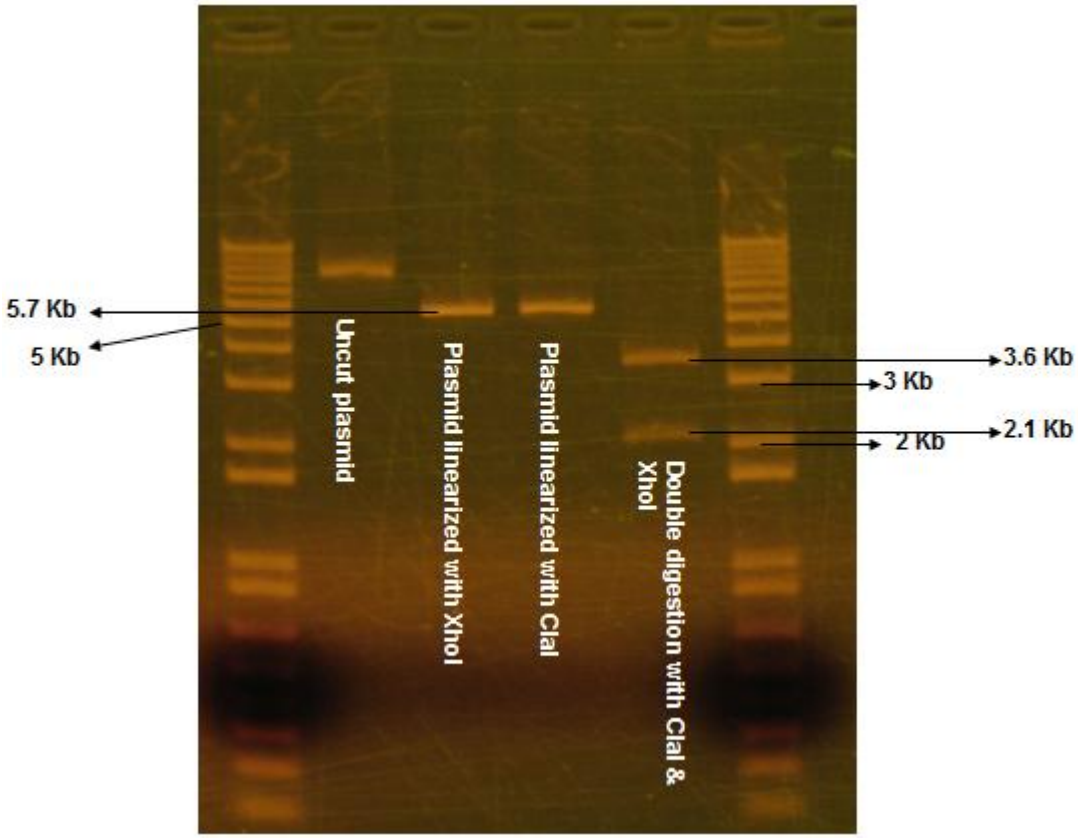

Figure 37: pBS595 plasmid confirmation digest

Figure 37 suggests that the linearized plasmid is around 5.7Kb. The restriction digestion with XhoI, MluI, and KpnI suggested a KpnI site 1800 bp upstream of the MluI site. Double digestion of the pBS595 plasmid with KpnI and MluI gave out the 1.8 Kb EGFP-Cre fusion fragment. This fragment was gel purified and was ready to be cloned into the pTRE-Tight vector provided by Clontech. The vector was digested with KpnI and MluI using buffer B at 37°C for 1 hour. The digested product was run on a 1% agarose gel and the required fragment was gel purified. The 5' KpnI ends and the 3' MluI ends of the vector and the insert were cloned together. The clone thus obtained was digested with

KpnI and MluI to confirm the presence of the 1.8 kb EGFP-Cre fusion gene. Figure 39 shows the gel picture of this digest.

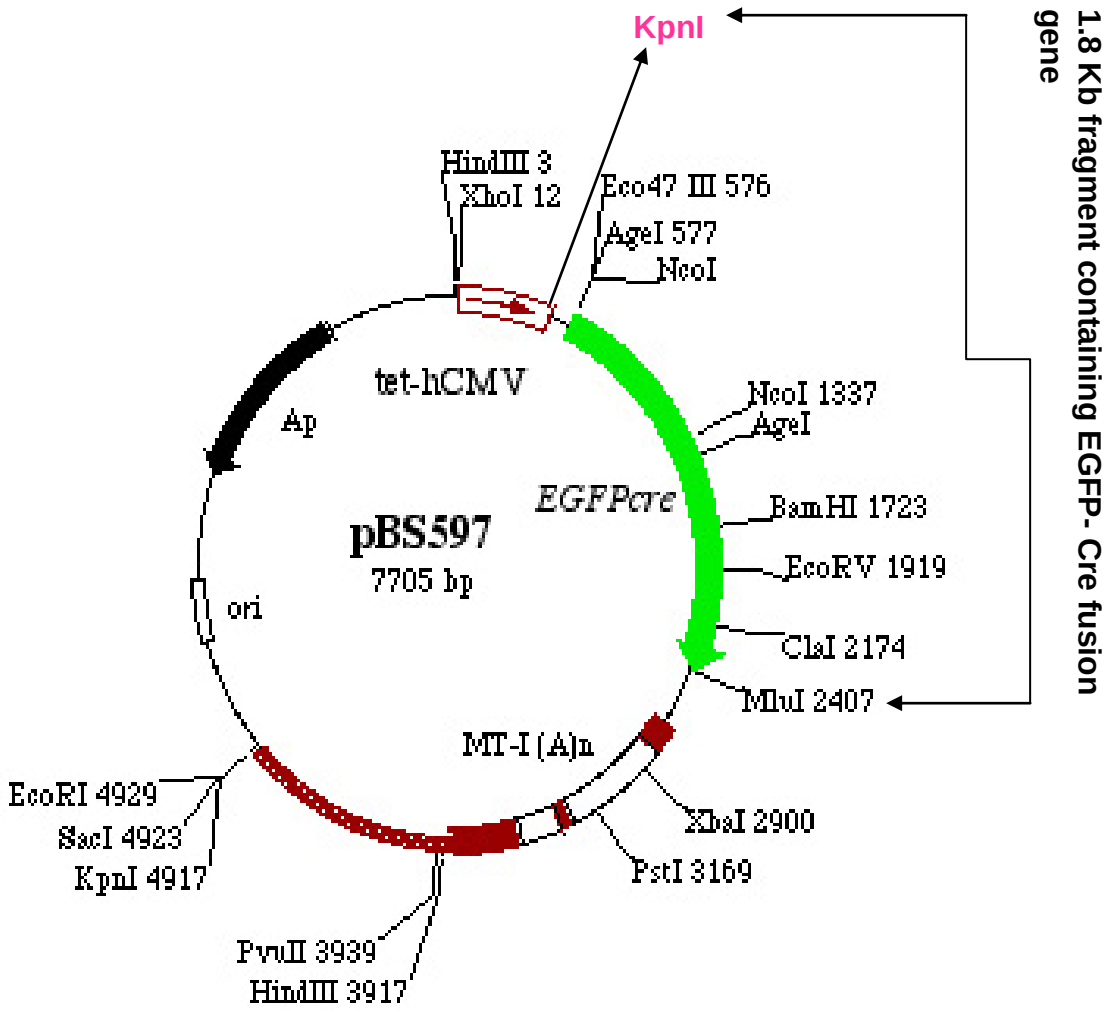

Figure 38: shows the 1.8 kb fragment between the KpnI and MluI site.

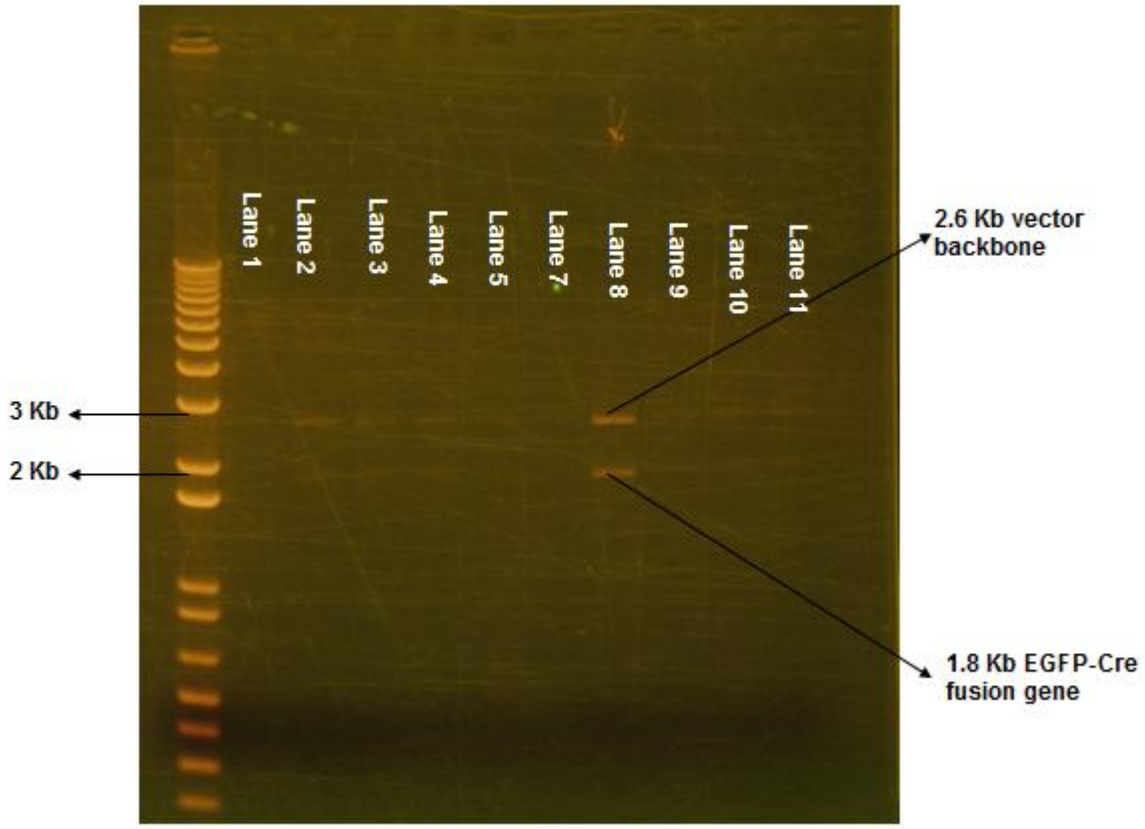

Figure 39: pTRE-Tight-Cre digestion to confirm presence of EGFP-Cre

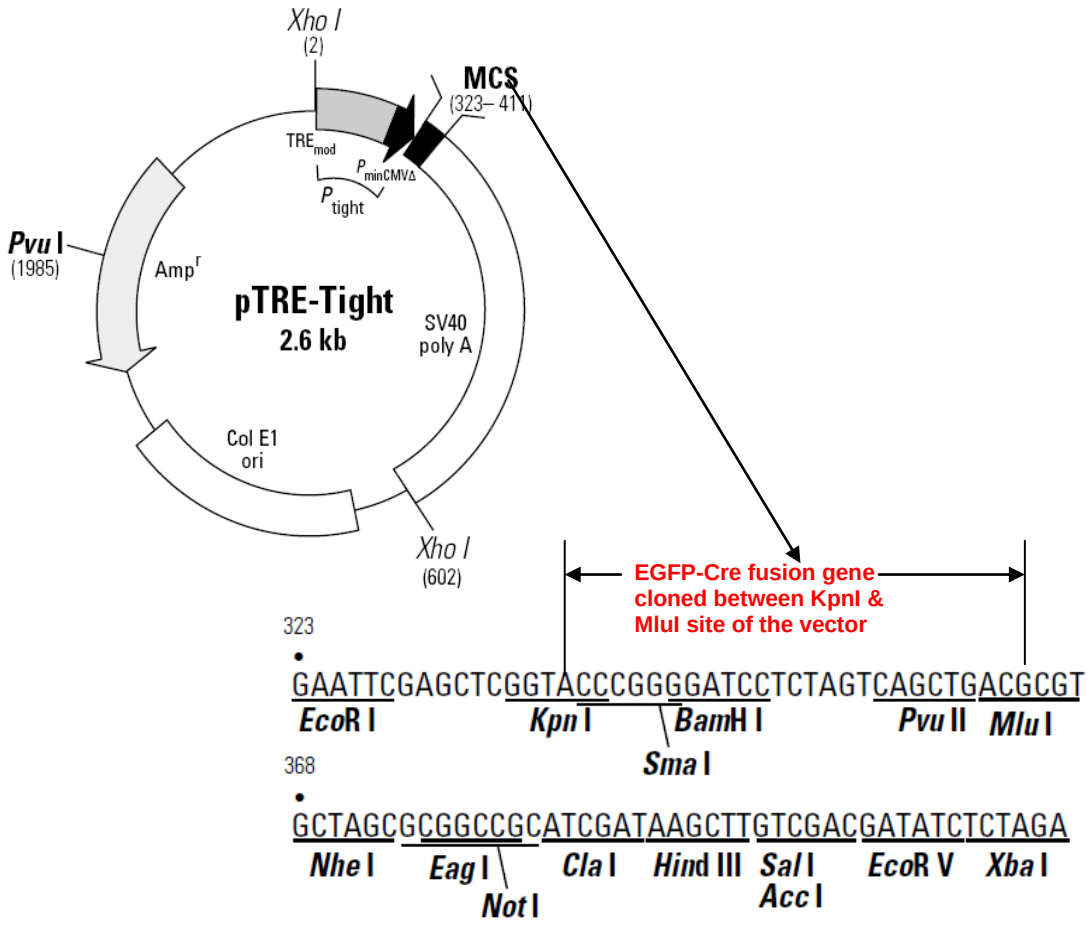

Figure 40: pTRE-Tight-EGFP-Cre cloning

Figure 40. shows the multiple cloning site of the pTRE-Tight vector into which the EGFP-Cre fusion gene has been cloned.

The clone was sequenced using the primer:

5'-AGG CGT ATC ACG AGG CCC TTT CGT-3'

Sequencing result:

TTAGTTCTCCTATAGTGATAGAGAACGTATGTCGAGTTTACTCCCTATCAGTGATAGAGAACGATGTC
GAGTTTACTCCCTATCAGTGATAGAGAACGTATGTCGAGTTTACTCCCTATCAGTGATAGAGAACGTA
TGTCGAGTTTACTCCCTATCAGTGATAGAGAACGTATGTCGAGTTTATCCCTATCAGTGATAGAGAAC
GTATGTCGAGTTTACTCCCTATCAGTGATAGAGAACGTATGTCGAGGTAGGCGTGTACGGTGGGAGGC
CTATATAAGCAGAGCTCGTTTAGTGAACCGTCAGATCGC
[CTGGAGAATTCGAGCTCGGTACCCGGGTCGAGGTAGGCGTGTACGGTGGGAGGC
EcoRI KpnI

CTA**TATAA**GCAGAGCTCGTTTAGTGAACCGTCAGATCGCCTGGAGACGCCATCCACGCTGTTTTGACC
TCCAT

AGAAGACACCGGGACCGATCCAGCCTCCGCGGCCCC**GAATTC**GAGCTCGGTACCCGGGGATCTGCAC
CGGTCGCCACC**]** EcoRI
ATGGTGAGCAAGGGCGAGGAGCTGTTCACCGGGGTGGTGCCCATCCTGGTCGAGCTGGA
CGGCGACGTAAACGGCCACAAGTTCAGCGTGTCCGGCGAGGGCGAGGGCGATGCCACCT
ACGGCAAGCTGACCCTGAAGTTCATCTGCACCACCGGCAAGCTGCCCGTGCCCTGGCCC
ACCCTCGTGACCACCCTGACCTACGGCGTGCAGTGCTTCAGCCGCTACCCCGACCACAT
GAAGCAGCACGACTTCTTCAAGTCCGCCATGCCCGAAGGCTACGTCCAGGAGCGCACCA
TCTTCTTCAAGGACGACGGCAACTACAAGACCCGCGCCGAGGTGAAGTTCGAGGGCGAC
ACCCTGGTGAACCGCATCGAGCTGAAGGGCATCGACTTCAAGGAGGACGGCAACATCCT
GGGGCACAAGCTGGAGTACAACTACAACAGCCACAACGTCTATATCATGGCCGACAAGC
AGAAGAACGGCATCAAGGTGAACTTC

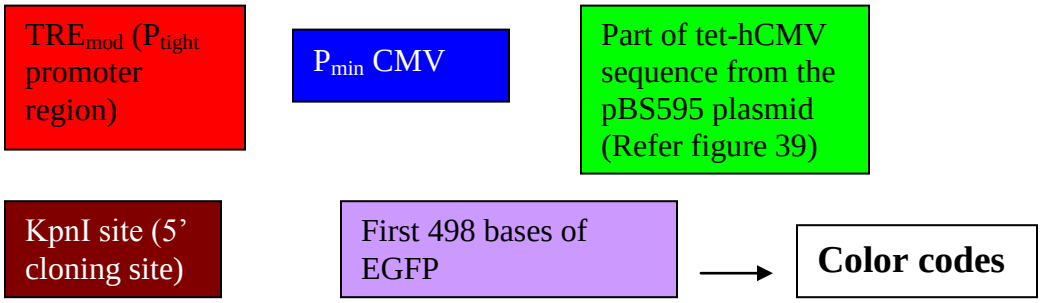

Figure 41: pTRE-Tight-Cre sequencing result

In Figure 41, the sequence shown in green is part of the tet-hCMV from the pBS595 plasmid. This sequence was excised out using EcoRI. This resulted in the final product:

pTRE-Tight-Cre

4.2) Tet-On regulated expression of pTRE-Tight-Cre in Hek293T cells.

Day1: Hek293T cells were seeded in a 6-well plate.

Day2: 24 hours from seeding, the cells reached 70% confluence. At this stage they were transiently transfected with CNPase-rtTA and TRE-Cre in a 1:1 ratio.

Day3: The cells were treated with various concentrations of doxycycline:

0, .01µg/ml, .05 µg/ml, 0.1 µg/ml, 0.5 µg/ml.

Day5: Cells were harvested and protein samples were analyzed by immunoblotting.

4.2b) GFP Expression

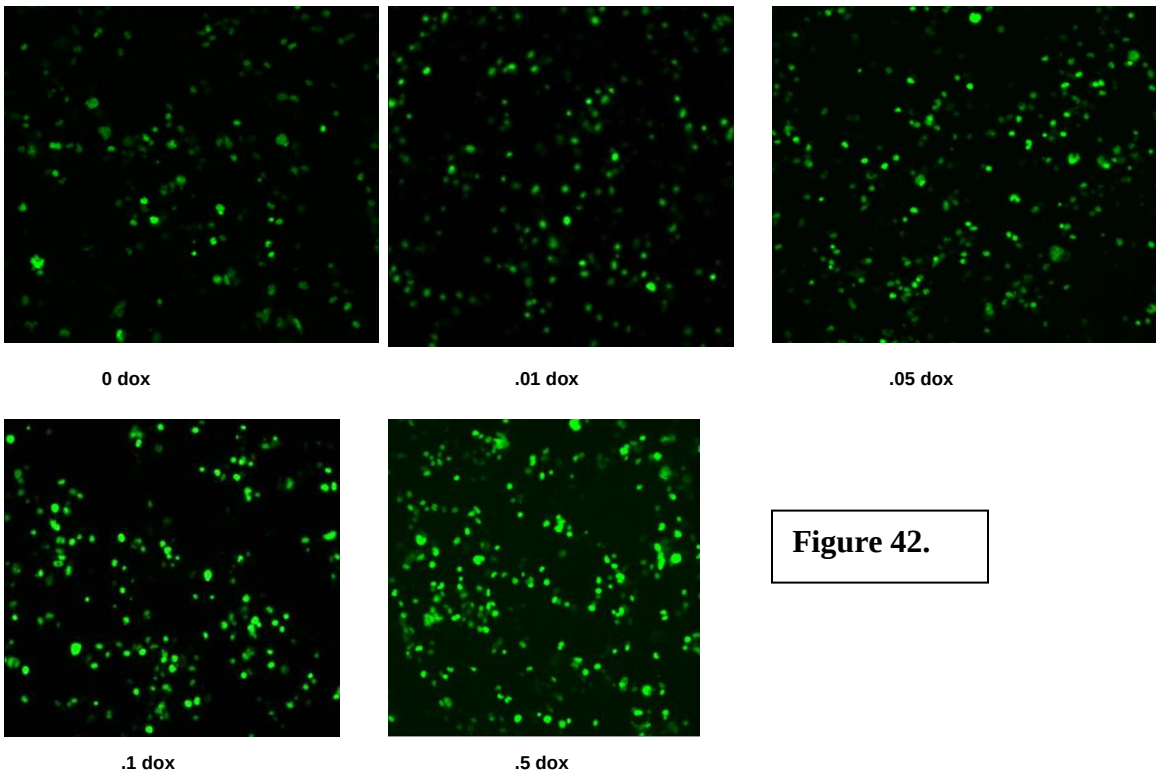

Figure 42.

Figure 42: GFP expression by pTRE-Tight-Cre

48 hours after drug treatment the GFP expression was observed at 40X magnification under an epifluorescence microscope. Shown above are the fluorescing cells at different doses of doxycycline (drug concentrations are in μg/ml). Unlike the dominant negative constructs mentioned in the previous sections, the cells transfected with pTRE-Tight-Cre fluoresced in the absence of Doxycycline.

4.2b) pTRE-Tight-Cre expression

Immunoblot analysis was carried out to determine the pTRE-Tight-Cre expression level at different concentrations of doxycycline. On day 5 of the experiment the transfected and drug treated Hek293T cells were harvested and their lysates were prepared for

immunoblot analysis. Samples were resolved by SDS-PAGE using a 10% acrylamide gel. Western blot was performed using a monoclonal antibody against Cre. The mouse monoclonal antibody against Cre was purchased from Abcam. Overnight incubation of the blot with the antibody (1:1000) at 4°C followed by chemiluminescent detection yielded the following result.

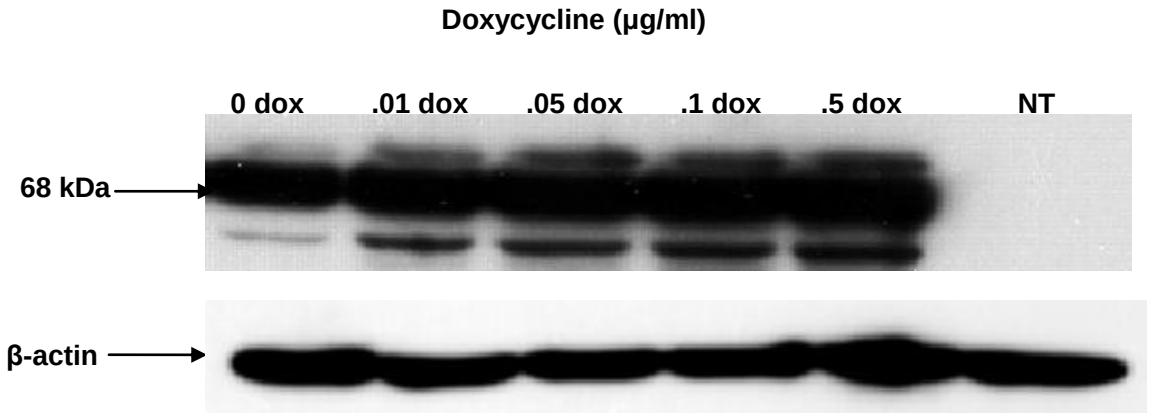

Figure 43.

As seen in the above immunoblot, the transgene pTRE-Tight-EGFP-Cre is induced even in the absence of Doxycycline. Such leaky expression could hamper the temporal regulation of the transgene expression. Hence, in order to reduce the leaky expression, the transfection ratio of the CNPase-rtTA transgene to the pTRE-Tight-EGFP-Cre transgene was varied; Cre transgene **:** rtTA transgene ⟶ 1:3, 1:10, 1:20. The following immunoblot was obtained using the above transfection ratios:

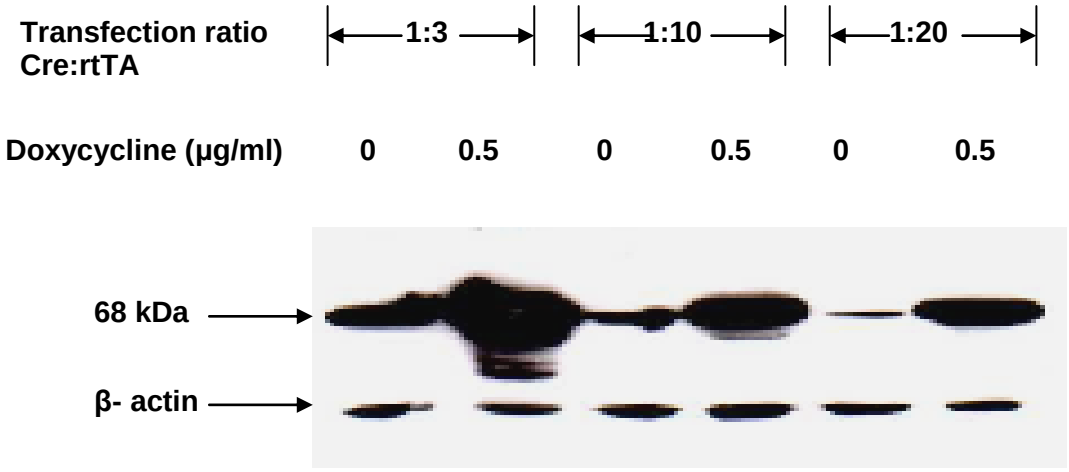

Figure 43a.

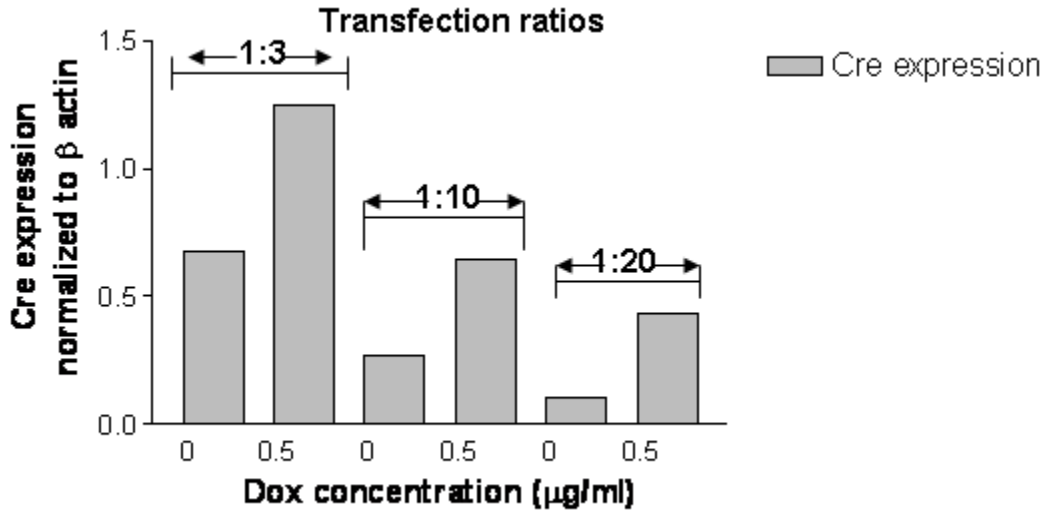

Figure 43b.

Figure 43: pTRE-Tight-Cre immunoblot analysis

Figure 43a shows the immunoblot obtained on transfecting the cells with greater amounts of the rtTA transgene compared to the Cre containing transgene. Since the purpose of this experiment was to reduce the residual Cre expression (in the absence of Dox), only two treatments were incorporated: 0 Dox and 0.5 µg/ml Dox. **Figure 43b** shows the immunoblot quantitation, wherein the pTRE-Tight-EGFP-CRE expression

levels were normalized to β-actin and plotted in the form of bar graphs. As seen in the graph, the basal Cre expression in the absence of Dox decreases, when transfected with lesser amounts of the Cre transgene.

Summary: The Cre expression is dependent on the transfection ratio of the CNPase-rtTA : Cre transgene, wherein least amount of basal Cre expression was observed in the cells transfected in a 1:20 ratio. The cells transfected in the ratio of 1:3 had 7 fold greater residual Cre expression when compared to the cells transfected in the ratio of 1:20. Though the residual expression reduced considerably using 1:20 transfection ratio, the induction in the 0.5 μg/ml Dox treated cells was much lesser when compared to the cells transfected in a 1:3 ratio.

III) DISCUSSION

Segmental demyelination is one of the basic patterns observed in the pathology of DPN. Demyelinating neuropathies primarily affect SCs and these myelinating cells undergo substantial degeneration in diabetic neuropathy. Hence, it is of pertinence to investigate possible mechanisms which may contribute to the demyelination of SCs and the progression of DPN.

Transgenic technologies have had a tremendous impact on biomedical research and human welfare[3]. Transgenic mice provide valuable experimental models to analyze gene function and regulation, and have emerged as one of the best overall gene function assay systems as the analysis is carried out on the whole organism. The study of gene function in such complex genetic environments would greatly profit from systems that would allow stringent control over the transgene expression. Integrating the

conventional transgene technology with the inducible expression systems would help exert a temporal and spatial control over the transgene expression. Therefore, this project generated three different Tet-On system based bi-transgenic vectors for use in generating novel mouse models for DPN research.

CNPase-rtTA; P_{tight} -DN-ErbB4: We used the dominant negative ErbB4 construct which blocks neuregulin signaling by binding NRG ligands and preventing them from binding to endogenous ErbB3, and ErbB4[73]. The rtTA was placed under the control of the SC-specific CNPase promoter in order to ensure the DN-ErbB4 expression in these myelinating cells.

One limitation in the use of mouse models of DPN is that, this species does not develop segmental demyelination which is a hallmark of the human disease. This may be due to the activation of NRG signaling promoting the myelinated phenotype. Therefore, the DN-ErbB4 bi-transgenic system has been developed in this project to investigate whether the transgene induction would help promote a diabetes-induced demyelination, since endogenous NRG signaling would be blocked.

Transgenic mice have been generated that express dominant negative ErbB4 receptor (DN-erbB4) under the control of the CNPase promoter [74], however, this animal model is limited by its reliance on the endogenous regulation of CNPase promoter activity. Our constructs would permit a temporal and spatial control over the transgene expression since it would be induced in the mice only in the presence of Dox. Thus, Dox would induce DN-ErbB4, which would block NRG signaling, resulting in a demyelinating phenotype in these mouse models of DPN. Removal of Dox from the diet of these mice might restore the NRG signaling, which could result in remyelination. In

light of the above and the evidence suggesting that reduction in the NRG1-ErbB signaling may be involved in the pathogenesis of peripheral neuropathies with hypomyelination, the DN-ErbB4 bi-transgenic system developed in this project would help further elucidate the role of ErbB receptor signaling, in myelinating SCs, with respect to DPN.

CNPase-rtTA; P_{tight} -dnUbc9: Evidence from studies underscore the therapeutic potential of heat shock proteins for demyelinating neuropathies[105]. It has been reported that EC137, a small-molecule inhibitor of HSP90, effectively enhances chaperone levels (HSP27, HSP70 and αB-crystallin) and improves myelination by SCs from neuropathic mice[105]. However, the precise molecular mechanism by which inhibition of HSP90 aids myelin formation remains unclear[105].

Preliminary data suggests that sumoylation may be a critical component in mediating the heat shock response. In light of the above evidence suggesting that the pharmacological induction of heat shock proteins improves myelination in neuropathic models, it has been hypothesized that sumoylation could be involved in the progression of DPN. Moreover, recent studies have indicated that the mitochondrial fission protein Drp1 may be a central regulator of neuropathies and that Drp1 undergoes sumoylation. These evidence corroborate the hypothesis that sumoylation could play a pivotal role in the pathogenesis of DPN.

Ubc9 is the sole E2 conjugating enzyme required for protein sumoylation[95], hence, inhibition of Ubc9 would throw light on sumoylation. Ubc9's involvement in regulating several critical pathways hampers researchers from knocking down this gene in order to study its functions. In *C.elegans* the Ubc9 knockdown proved

to be lethal. Additionally, Ubc9 deficient mice generated using the flox-and-invert strategy also had the embryonic lethal phenotype. On the whole, in yeast and higher eukaryotic cells, gene disruption of Ubc9 has been reported to be lethal[101-102]. This deficiency can be obviated by using a dominant negative form of Ubc9 under the control of the Tet-On regulatory system.

We used a substitution mutant of Ubc9 (C93S), which exhibits a dominant inhibitory effect on the endogenous Ubc9. The bi-transgenic system, Cnpase-rtTA; P_{tight} -dnUbc9, would permit a temporal and spatial control over the transgene expression since it would be induced in the mice only in the presence of Dox. As the rtTA is placed under the control of the SC-specific CNPase promoter, the dnUbc9 would express in SCs which would interfere with sumoylation and permit us to assess the role of this post-translational modification in DPN.

CNPase-rtTA; P_{tight} -Cre: The Cre lox technology is often used in the generation of knockout and conditional knockout animals. Integrating this technology with the Tet-On system would help to have a temporal control over the deletion of the gene of interest. We developed the above mentioned transgenes in order to generate a bi-transgenic mouse which can be crossed with a mouse having the gene of interest flanked by loxP sites. Since rtTA is placed under the control of the CNPase promoter, Cre recombinase would be expressed in SCs, which would delete the gene of interest in these cells in the presence of Dox. Therefore, this model could be used for the conditional deletion of genes associated with DPN. Deletion of such genes specifically in myelinating SCs would help explore their role with respect to DPN.

Placement of genes under the control of the rtTA- P_{tight} system has been shown to display excellent dose-response characteristics, which allows not only a qualitative off-on transition but also a fine tuning of gene expression and the study of quantitative aspects of gene activity. The transgenes constructed in this project were validated in Hek293T cells to ensure if they expressed in a tight and highly inducible manner. The transgene transfected cell lines when treated with Dox showed a dose-dependent expression of the gene of interest. Maximum gene induction was observed when treated with 0.5μg/ml Dox, wherein, there was low or minimal basal expression in the absence of Dox was. Thus, consistent with results from previous studies using the Tet-On system, the bi-transgenic system developed in this project works in a tight and highly inducible manner in Hek293T cells. Though Dox induced high levels of transgene expression, it is yet to be seen if the induction is sufficient to display the desired function. Therefore, it is essential to perform assays to validate the functionality of this system.

On testing the CNPase-rtTA and P_{tight} -Cre transgenes in Hek293T cells, it was found that there was basal level Cre expression in the absence of Dox. In order to circumvent this issue the transgenes were transfected in varying ratios. Even though the basal expression of the Cre transgene was reduced when transfected in a 1:20 ratio (rtTA: Cre), the maximum induction by Dox was compromised too. Hence, it is necessary to ensure that lowering the Cre transfection ratio did not compromise the function of the recombinase. The following functional assay is currently being developed to validate the above. Cells have been stably transfected with the plox plasmid containing a floxed neomycin resistance gene. The cells will then be stably transfected with the CNPase-rtTA and P_{tight}-Cre transgenes, and treated with Dox. If the Cre recombinase is induced

sufficiently, then this recombinase would cleave the plox plasmid at the loxP sites, which in turn would delete the neomycin resistance gene. When maintained in a media containing Geneticin, these cells would die due to the lack of the neomycin resistance gene. Massive cell death would confirm that the recombinase is induced sufficiently by Dox. Absence of cell death in the untreated cells would confirm that the system has low or minimal residual expression.

This project showed that the three Tet-On regulated bi-transgenic models of this study express the transgenes in a tight and highly induced manner in Hek293T cells. Future directions must include the development of assays in order to validate the functioning of the transgenes. Moreover, the CNPase promoter sequence used in this project, to drive the expression of rtTA, is yet to be tested for its specific expression in Schwann cells. The transgenes could be validated in isolated Schwann cells to confirm the same. However, even if the transgenes function efficiently in vitro, the same can not be guaranteed in vivo. Therefore, the results of this project reflect that it might prove lucrative to pursue the development of bi-transgenic mice using these transgenes, however, conclusive deductions with respect to the functioning of these transgenes can only be drawn once the mice models are generated.

IV References

1. Jaenisch, R. and B. Mintz, *Simian virus 40 DNA sequences in DNA of healthy adult mice derived from preimplantation blastocysts injected with viral DNA.* Proc Natl Acad Sci U S A, 1974. **71**(4): p. 1250-4.
2. Transgenicmouse.com, *Transgenic Mouse.* 2005.
3. Gama Sosa, M.A., R. De Gasperi, and G.A. Elder, *Animal transgenesis: an overview.* Brain Struct Funct, 2009.
4. Chesselet, M.F., *Animal models of neurological disorders.* NeuroRx, 2005. **2**(3): p. 395.
5. Wong, P.C., et al., *Genetically engineered mouse models of neurodegenerative diseases.* Nat Neurosci, 2002. **5**(7): p. 633-9.
6. Notarianni, *Embryonic stem cells: a practical approach.* Oxford University Press, Oxford, 2006.
7. Joyner, *Gene targeting: a practical approach.* Oxford University Press, Oxford; New York, 2000.
8. Gordon, J.W., et al., *Genetic transformation of mouse embryos by microinjection of purified DNA.* Proc Natl Acad Sci U S A, 1980. **77**(12): p. 7380-4.
9. Kozak, M., *An analysis of 5'-noncoding sequences from 699 vertebrate messenger RNAs.* Nucleic Acids Res, 1987. **15**(20): p. 8125-48.
10. Goodwin, E.C. and F.M. Rottman, *The 3'-flanking sequence of the bovine growth hormone gene contains novel elements required for efficient and accurate polyadenylation.* J Biol Chem, 1992. **267**(23): p. 16330-4.
11. genOway.com, *Technology-Pro-nuclear injection.* 2006.
12. Potts, W., et al., *Chicken beta-globin 5'HS4 insulators function to reduce variability in transgenic founder mice.* Biochem Biophys Res Commun, 2000. **273**(3): p. 1015-8.
13. Giraldo, P., et al., *The potential benefits of insulators on heterologous constructs in transgenic animals.* Transgenic Res, 2003. **12**(6): p. 751-5.
14. De Gasperi, R., et al., *The IRG mouse: A two-color fluorescent reporter for assessing Cre-mediated recombination and imaging complex cellular relationships in situ.* Genesis, 2008. **46**(6): p. spcone.
15. Paillard, F., *"Tet-on": a gene switch for the exogenous regulation of transgene expression.* Hum Gene Ther, 1998. **9**(7): p. 983-5.
16. Gossen, M. and H. Bujard, *Tight control of gene expression in mammalian cells by tetracycline-responsive promoters.* Proc Natl Acad Sci U S A, 1992. **89**(12): p. 5547-51.
17. Mayo, K.E., R. Warren, and R.D. Palmiter, *The mouse metallothionein-I gene is transcriptionally regulated by cadmium following transfection into human or mouse cells.* Cell, 1982. **29**(1): p. 99-108.

18. Palmiter, R.D., et al., *Dramatic growth of mice that develop from eggs microinjected with metallothionein-growth hormone fusion genes.* Nature, 1982. **300**(5893): p. 611-5.
19. Hillen, Protein-Nucleic Acid Interaction, 1989.
20. Gossen, M., et al., *Transcriptional activation by tetracyclines in mammalian cells.* Science, 1995. **268**(5218): p. 1766-9.
21. Clontech Laboratories, I., *Tet-Off and Tet-On Gene Expression Systems User Manual.* 2005.
22. Triezenberg, S.J., R.C. Kingsbury, and S.L. McKnight, *Functional dissection of VP16, the trans-activator of herpes simplex virus immediate early gene expression.* Genes Dev, 1988. **2**(6): p. 718-29.
23. Swiger, R.R., J.D. Tucker, and J.A. Heddle, *Detection of transgenic animals without cell culture using fluorescence in situ hybridization.* Biotechniques, 1995. **18**(6): p. 952-4, 956, 958.
24. Shi, Y.P., et al., *The mapping of transgenes by fluorescence in situ hybridization on G-banded mouse chromosomes.* Mamm Genome, 1994. **5**(6): p. 337-41.
25. Schmidt, C., et al., *Mapping of candidate genes for hypertension by fluorescence in situ hybridization on the genome of transgenic rats and mice.* Clin Exp Hypertens, 1998. **20**(2): p. 185-204.
26. NIDDK, *Diabetic Neuropathies: The Nerve Damage of Diabetes.* 2009.
27. McGuire, J.F., et al., *Caveolin-1 and altered neuregulin signaling contribute to the pathophysiological progression of diabetic peripheral neuropathy.* Diabetes, 2009. **58**(11): p. 2677-86.
28. Agamanolis, D.P., *Peripheral Nerve Pathology.* Neuropathology, 2007.
29. Yu, C., S. Rouen, and R.T. Dobrowsky, *Hyperglycemia and downregulation of caveolin-1 enhance neuregulin-induced demyelination.* Glia, 2008. **56**(8): p. 877-87.
30. Braun, P.E., et al., *Immunocytochemical localization by electron microscopy of 2'3'-cyclic nucleotide 3'-phosphodiesterase in developing oligodendrocytes of normal and mutant brain.* J Neurosci, 1988. **8**(8): p. 3057-66.
31. Kursula, P., *Structural properties of proteins specific to the myelin sheath.* Amino Acids, 2008. **34**(2): p. 175-85.
32. Sakamoto, Y., et al., *Crystal structure of the catalytic fragment of human brain 2',3'-cyclic-nucleotide 3'-phosphodiesterase.* J Mol Biol, 2005. **346**(3): p. 789-800.
33. Kasama-Yoshida, H., et al., *A comparative study of 2',3'-cyclic-nucleotide 3'-phosphodiesterase in vertebrates: cDNA cloning and amino acid sequences for chicken and bullfrog enzymes.* J Neurochem, 1997. **69**(4): p. 1335-42.
34. Sprinkle, T.J., M.E. Zaruba, and G.M. McKhann, *Activity of 2',3'-cyclic-nucleotide 3'-phosphodiesterase in regions of rat brain during development: quantitative relationship to myelin basic protein.* J Neurochem, 1978. **30**(2): p. 309-14.
35. Braun, P.E. and R.L. Barchi, *2',3'-cyclic nucleotide 3'-phosphodiesterase in the nervous system. Electrophoretic properties and developmental studies.* Brain Res, 1972. **40**(2): p. 437-44.
36. Olafson, R.W., G.I. Drummond, and J.F. Lee, *Studies on 2',3'-cyclic nucleotide-3'-phosphohydrolase from brain.* Can J Biochem, 1969. **47**(10): p. 961-6.

37. Kurihara, T. and Y. Tsukada, *The regional and subcellular distribution of 2',3'-cyclic nucleotide 3'-phosphohydrolase in the central nervous system.* J Neurochem, 1967. **14**(12): p. 1167-74.
38. Weissbarth, S., et al., *The activity of 2',3'-cyclic nucleotide 3'-phosphodiesterase in rat tissues.* J Neurochem, 1981. **37**(3): p. 677-80.
39. Sprinkle, T.J., *2',3'-cyclic nucleotide 3'-phosphodiesterase, an oligodendrocyte-Schwann cell and myelin-associated enzyme of the nervous system.* Crit Rev Neurobiol, 1989. **4**(3): p. 235-301.
40. Braun, P.E., et al., *Isoprenoid modification permits 2',3'-cyclic nucleotide 3'-phosphodiesterase to bind to membranes.* J Neurosci Res, 1991. **30**(3): p. 540-4.
41. Gravel, M., et al., *Overexpression of 2',3'-cyclic nucleotide 3'-phosphodiesterase in transgenic mice alters oligodendrocyte development and produces aberrant myelination.* Mol Cell Neurosci, 1996. **7**(6): p. 453-66.
42. Vlkolinsky, R., et al., *Decreased brain levels of 2',3'-cyclic nucleotide-3'-phosphodiesterase in Down syndrome and Alzheimer's disease.* Neurobiol Aging, 2001. **22**(4): p. 547-53.
43. Sloane, J.A., et al., *Age-dependent myelin degeneration and proteolysis of oligodendrocyte proteins is associated with the activation of calpain-1 in the rhesus monkey.* J Neurochem, 2003. **84**(1): p. 157-68.
44. Muraro, P.A., et al., *T cell response to 2',3'-cyclic nucleotide 3'-phosphodiesterase (CNPase) in multiple sclerosis patients.* J Neuroimmunol, 2002. **130**(1-2): p. 233-42.
45. Lappe-Siefke, C., et al., *Disruption of Cnp1 uncouples oligodendroglial functions in axonal support and myelination.* Nat Genet, 2003. **33**(3): p. 366-74.
46. O'Neill, R.C., et al., *CNP2 mRNA directs synthesis of both CNP1 and CNP2 polypeptides.* J Neurosci Res, 1997. **50**(2): p. 248-57.
47. Kurihara, T., et al., *Alternative splicing of mouse brain 2',3'-cyclic-nucleotide 3'-phosphodiesterase mRNA.* Biochem Biophys Res Commun, 1990. **170**(3): p. 1074-81.
48. Douglas, A.J., et al., *Structure and chromosomal localization of the human 2',3'-cyclic nucleotide 3'-phosphodiesterase gene.* Ann Hum Genet, 1992. **56**(Pt 3): p. 243-54.
49. Gravel, M., D. DeAngelis, and P.E. Braun, *Molecular cloning and characterization of rat brain 2',3'-cyclic nucleotide 3'-phosphodiesterase isoform 2.* J Neurosci Res, 1994. **38**(3): p. 243-7.
50. Monoh, K., et al., *Structure of mouse 2',3'-cyclic-nucleotide 3'-phosphodiesterase gene.* Biochem Biophys Res Commun, 1989. **165**(3): p. 1213-20.
51. Bernier, L., et al., *Molecular cloning of a 2',3'-cyclic nucleotide 3'-phosphodiesterase: mRNAs with different 5' ends encode the same set of proteins in nervous and lymphoid tissues.* J Neurosci, 1987. **7**(9): p. 2703-10.
52. Monoh, K., et al., *Structure, expression and chromosomal localization of the gene encoding human 2',3'-cyclic-nucleotide 3'-phosphodiesterase.* Gene, 1993. **129**(2): p. 297-301.
53. Gravel, M., et al., *Four-kilobase sequence of the mouse CNP gene directs spatial and temporal expression of lacZ in transgenic mice.* J Neurosci Res, 1998. **53**(4): p. 393-404.

54. Bublil, E.M. and Y. Yarden, *The EGF receptor family: spearheading a merger of signaling and therapeutics.* Curr Opin Cell Biol, 2007. **19**(2): p. 124-34.
55. Olayioye, M.A., et al., *The ErbB signaling network: receptor heterodimerization in development and cancer.* EMBO J, 2000. **19**(13): p. 3159-67.
56. Holmes, W.E., et al., *Identification of heregulin, a specific activator of p185erbB2.* Science, 1992. **256**(5060): p. 1205-10.
57. Peles, E., et al., *Isolation of the neu/HER-2 stimulatory ligand: a 44 kd glycoprotein that induces differentiation of mammary tumor cells.* Cell, 1992. **69**(1): p. 205-16.
58. Wen, D., et al., *Neu differentiation factor: a transmembrane glycoprotein containing an EGF domain and an immunoglobulin homology unit.* Cell, 1992. **69**(3): p. 559-72.
59. Falls, D.L., et al., *ARIA, a protein that stimulates acetylcholine receptor synthesis, is a member of the neu ligand family.* Cell, 1993. **72**(5): p. 801-15.
60. Marchionni, M.A., et al., *Glial growth factors are alternatively spliced erbB2 ligands expressed in the nervous system.* Nature, 1993. **362**(6418): p. 312-8.
61. Busfield, S.J., et al., *Characterization of a neuregulin-related gene, Don-1, that is highly expressed in restricted regions of the cerebellum and hippocampus.* Mol Cell Biol, 1997. **17**(7): p. 4007-14.
62. Carraway, K.L., 3rd, et al., *Neuregulin-2, a new ligand of ErbB3/ErbB4-receptor tyrosine kinases.* Nature, 1997. **387**(6632): p. 512-6.
63. Chang, H., et al., *Ligands for ErbB-family receptors encoded by a neuregulin-like gene.* Nature, 1997. **387**(6632): p. 509-12.
64. Harari, D., et al., *Neuregulin-4: a novel growth factor that acts through the ErbB-4 receptor tyrosine kinase.* Oncogene, 1999. **18**(17): p. 2681-9.
65. Zhang, D., et al., *Neuregulin-3 (NRG3): a novel neural tissue-enriched protein that binds and activates ErbB4.* Proc Natl Acad Sci U S A, 1997. **94**(18): p. 9562-7.
66. Lopez-Bendito, G., et al., *Tangential neuronal migration controls axon guidance: a role for neuregulin-1 in thalamocortical axon navigation.* Cell, 2006. **125**(1): p. 127-42.
67. Flames, N., et al., *Short- and long-range attraction of cortical GABAergic interneurons by neuregulin-1.* Neuron, 2004. **44**(2): p. 251-61.
68. Mei, L. and W.C. Xiong, *Neuregulin 1 in neural development, synaptic plasticity and schizophrenia.* Nat Rev Neurosci, 2008. **9**(6): p. 437-52.
69. Burden, S. and Y. Yarden, *Neuregulins and their receptors: a versatile signaling module in organogenesis and oncogenesis.* Neuron, 1997. **18**(6): p. 847-55.
70. Adlkofer, K. and C. Lai, *Role of neuregulins in glial cell development.* Glia, 2000. **29**(2): p. 104-11.
71. Buonanno, A. and G.D. Fischbach, *Neuregulin and ErbB receptor signaling pathways in the nervous system.* Curr Opin Neurobiol, 2001. **11**(3): p. 287-96.
72. Rio, C., et al., *Neuregulin and erbB receptors play a critical role in neuronal migration.* Neuron, 1997. **19**(1): p. 39-50.
73. Roy, K., et al., *Loss of erbB signaling in oligodendrocytes alters myelin and dopaminergic function, a potential mechanism for neuropsychiatric disorders.* Proc Natl Acad Sci U S A, 2007. **104**(19): p. 8131-6.

74. Chen, S., et al., *Neuregulin 1-erbB signaling is necessary for normal myelination and sensory function.* J Neurosci, 2006. **26**(12): p. 3079-86.
75. Prevot, V., et al., *Activation of erbB-1 signaling in tanycytes of the median eminence stimulates transforming growth factor beta1 release via prostaglandin E2 production and induces cell plasticity.* J Neurosci, 2003. **23**(33): p. 10622-32.
76. Haugen, D.R., et al., *Expression of c-erbB-3 and c-erbB-4 proteins in papillary thyroid carcinomas.* Cancer Res, 1996. **56**(6): p. 1184-8.
77. Kew, T.Y., et al., *c-erbB-4 protein expression in human breast cancer.* Br J Cancer, 2000. **82**(6): p. 1163-70.
78. Savonenko, A.V., et al., *Alteration of BACE1-dependent NRG1/ErbB4 signaling and schizophrenia-like phenotypes in BACE1-null mice.* Proc Natl Acad Sci U S A, 2008. **105**(14): p. 5585-90.
79. Gerlai, R., P. Pisacane, and S. Erickson, *Heregulin, but not ErbB2 or ErbB3, heterozygous mutant mice exhibit hyperactivity in multiple behavioral tasks.* Behav Brain Res, 2000. **109**(2): p. 219-27.
80. Golub, M.S., S.L. Germann, and K.C. Lloyd, *Behavioral characteristics of a nervous system-specific erbB4 knock-out mouse.* Behav Brain Res, 2004. **153**(1): p. 159-70.
81. Rimer, M., et al., *Neuregulin-1 immunoglobulin-like domain mutant mice: clozapine sensitivity and impaired latent inhibition.* Neuroreport, 2005. **16**(3): p. 271-5.
82. Stefansson, H., et al., *Neuregulin 1 and susceptibility to schizophrenia.* Am J Hum Genet, 2002. **71**(4): p. 877-92.
83. Penington, D.J., I. Bryant, and D.J. Riese, 2nd, *Constitutively active ErbB4 and ErbB2 mutants exhibit distinct biological activities.* Cell Growth Differ, 2002. **13**(6): p. 247-56.
84. Guertin, A.D., et al., *Microanatomy of axon/glial signaling during Wallerian degeneration.* J Neurosci, 2005. **25**(13): p. 3478-87.
85. Yasugi, T. and P.M. Howley, *Identification of the structural and functional human homolog of the yeast ubiquitin conjugating enzyme UBC9.* Nucleic Acids Res, 1996. **24**(11): p. 2005-10.
86. Entrez, *UBE2I; GeneID: 7329.* NCBI Entrez Gene.
87. Kovalenko, O.V., et al., *Mammalian ubiquitin-conjugating enzyme Ubc9 interacts with Rad51 recombination protein and localizes in synaptonemal complexes.* Proc Natl Acad Sci U S A, 1996. **93**(7): p. 2958-63.
88. Knipscheer, P., *Divide and conquer: the E2 active site.* NATURE STRUCTURAL & MOLECULAR BIOLOGY, 2006. **13**(6).
89. Ardley, H.C. and P.A. Robinson, *E3 ubiquitin ligases.* Essays Biochem, 2005. **41**: p. 15-30.
90. Hochstrasser, M., *SP-RING for SUMO: new functions bloom for a ubiquitin-like protein.* Cell, 2001. **107**(1): p. 5-8.
91. Jackson, P.K., et al., *The lore of the RINGs: substrate recognition and catalysis by ubiquitin ligases.* Trends Cell Biol, 2000. **10**(10): p. 429-39.
92. Reverter, D. and C.D. Lima, *Insights into E3 ligase activity revealed by a SUMO-RanGAP1-Ubc9-Nup358 complex.* Nature, 2005. **435**(7042): p. 687-92.

93. Zheng, N., et al., *Structure of a c-Cbl-UbcH7 complex: RING domain function in ubiquitin-protein ligases.* Cell, 2000. **102**(4): p. 533-9.
94. Zhang, M., et al., *Chaperoned ubiquitylation--crystal structures of the CHIP U box E3 ubiquitin ligase and a CHIP-Ubc13-Uev1a complex.* Mol Cell, 2005. **20**(4): p. 525-38.
95. Schwarz, S.E., et al., *The ubiquitin-like proteins SMT3 and SUMO-1 are conjugated by the UBC9 E2 enzyme.* Proc Natl Acad Sci U S A, 1998. **95**(2): p. 560-4.
96. Hay, R.T., *SUMO: a history of modification.* Mol Cell, 2005. **18**(1): p. 1-12.
97. Rodriguez, M.S., et al., *Nuclear retention of IkappaBalpha protects it from signal-induced degradation and inhibits nuclear factor kappaB transcriptional activation.* J Biol Chem, 1999. **274**(13): p. 9108-15.
98. Schmidt, D. and S. Muller, *Members of the PIAS family act as SUMO ligases for c-Jun and p53 and repress p53 activity.* Proc Natl Acad Sci U S A, 2002. **99**(5): p. 2872-7.
99. Gostissa, M., et al., *Activation of p53 by conjugation to the ubiquitin-like protein SUMO-1.* EMBO J, 1999. **18**(22): p. 6462-71.
100. Shen, Z., et al., *UBL1, a human ubiquitin-like protein associating with human RAD51/RAD52 proteins.* Genomics, 1996. **36**(2): p. 271-9.
101. Seufert, W., B. Futcher, and S. Jentsch, *Role of a ubiquitin-conjugating enzyme in degradation of S- and M-phase cyclins.* Nature, 1995. **373**(6509): p. 78-81.
102. Hayashi, T., et al., *Ubc9 is essential for viability of higher eukaryotic cells.* Exp Cell Res, 2002. **280**(2): p. 212-21.
103. Giorgino, F., et al., *The sentrin-conjugating enzyme mUbc9 interacts with GLUT4 and GLUT1 glucose transporters and regulates transporter levels in skeletal muscle cells.* Proc Natl Acad Sci U S A, 2000. **97**(3): p. 1125-30.
104. Sarge, K.D. and O.K. Park-Sarge, *Sumoylation and human disease pathogenesis.* Trends Biochem Sci, 2009. **34**(4): p. 200-5.
105. Rangaraju, S., et al., *Pharmacological induction of the heat shock response improves myelination in a neuropathic model.* Neurobiol Dis, 2008. **32**(1): p. 105-15.
106. Hilgarth, R.S., et al., *Insights into the regulation of heat shock transcription factor 1 SUMO-1 modification.* Biochem Biophys Res Commun, 2003. **303**(1): p. 196-200.
107. Cotto, J.J. and R.I. Morimoto, *Stress-induced activation of the heat-shock response: cell and molecular biology of heat-shock factors.* Biochem Soc Symp, 1999. **64**: p. 105-18.
108. Morano, K.A. and D.J. Thiele, *Heat shock factor function and regulation in response to cellular stress, growth, and differentiation signals.* Gene Expr, 1999. **7**(4-6): p. 271-82.
109. Hong, Y., et al., *Regulation of heat shock transcription factor 1 by stress-induced SUMO-1 modification.* J Biol Chem, 2001. **276**(43): p. 40263-7.
110. Edwards, J.L., et al., *Diabetes regulates mitochondrial biogenesis and fission in mouse neurons.* Diabetologia, 2010. **53**(1): p. 160-9.

111. Leinninger, G.M., et al., *Mitochondria in DRG neurons undergo hyperglycemic mediated injury through Bim, Bax and the fission protein Drp1.* Neurobiol Dis, 2006. **23**(1): p. 11-22.
112. Wang, X., et al., *Dynamin-like protein 1 reduction underlies mitochondrial morphology and distribution abnormalities in fibroblasts from sporadic Alzheimer's disease patients.* Am J Pathol, 2008. **173**(2): p. 470-82.
113. Men, X., et al., *Dynamin-related protein 1 mediates high glucose induced pancreatic beta cell apoptosis.* Int J Biochem Cell Biol, 2009. **41**(4): p. 879-90.
114. Figueroa-Romero, C., et al., *SUMOylation of the mitochondrial fission protein Drp1 occurs at multiple nonconsensus sites within the B domain and is linked to its activity cycle.* FASEB J, 2009. **23**(11): p. 3917-27.
115. Nagy, A., *Cre recombinase: the universal reagent for genome tailoring.* Genesis, 2000. **26**(2): p. 99-109.
116. Van Duyne, G.D., *A structural view of cre-loxp site-specific recombination.* Annu Rev Biophys Biomol Struct, 2001. **30**: p. 87-104.
117. Pechisker, A., *TARGETING YOUR DNA WITH THE CRE/LOX SYSTEM.* The Science Creative Quarterly, 2004(4).
118. Sternberg, N., et al., *Site-specific recombination and its role in the life cycle of bacteriophage P1.* Cold Spring Harb Symp Quant Biol, 1981. **45 Pt 1**: p. 297-309.
119. Gopaul, D.N., F. Guo, and G.D. Van Duyne, *Structure of the Holliday junction intermediate in Cre-loxP site-specific recombination.* EMBO J, 1998. **17**(14): p. 4175-87.
120. Robins, D.M., R. Axel, and A.S. Henderson, *Chromosome structure and DNA sequence alterations associated with mutation of transformed genes.* J Mol Appl Genet, 1981. **1**(3): p. 191-203.
121. Robins, D.M., et al., *Transforming DNA integrates into the host chromosome.* Cell, 1981. **23**(1): p. 29-39.
122. Scangos, G. and F.H. Ruddle, *Mechanisms and applications of DNA-mediated gene transfer in mammalian cells - a review.* Gene, 1981. **14**(1-2): p. 1-10.
123. Shapira, G., et al., *Novel use of synthetic oligonucleotide insertion mutants for the study of homologous recombination in mammalian cells.* Proc Natl Acad Sci U S A, 1983. **80**(15): p. 4827-31.
124. Smith, A.J. and P. Berg, *Homologous recombination between defective neo genes in mouse 3T6 cells.* Cold Spring Harb Symp Quant Biol, 1984. **49**: p. 171-81.
125. Smithies, O., et al., *Insertion of DNA sequences into the human chromosomal beta-globin locus by homologous recombination.* Nature, 1985. **317**(6034): p. 230-4.
126. Araki, K., et al., *Efficiency of recombination by Cre transient expression in embryonic stem cells: comparison of various promoters.* J Biochem, 1997. **122**(5): p. 977-82.
127. de Wit, T., D. Drabek, and F. Grosveld, *Microinjection of cre recombinase RNA induces site-specific recombination of a transgene in mouse oocytes.* Nucleic Acids Res, 1998. **26**(2): p. 676-8.
128. Ringrose, L., et al., *Comparative kinetic analysis of FLP and cre recombinases: mathematical models for DNA binding and recombination.* J Mol Biol, 1998. **284**(2): p. 363-84.

129. Blakely, G., et al., *Two related recombinases are required for site-specific recombination at dif and cer in E. coli K12.* Cell, 1993. **75**(2): p. 351-61.
130. Department of Biology, D.C., *Cre-lox P Recombination.* 2002.
131. JacksonLaboratory, *Introduction to Cre-lox technology.* 2010.
132. Sauer, B., *Conditional Gene Knockout Using Cre Recombinase.* Molecular Biotechnology, 2001. **17**.
133. Sauer, B. and N. Henderson, *Site-specific DNA recombination in mammalian cells by the Cre recombinase of bacteriophage P1.* Proc Natl Acad Sci U S A, 1988. **85**(14): p. 5166-70.
134. Gu, H., et al., *Deletion of a DNA polymerase beta gene segment in T cells using cell type-specific gene targeting.* Science, 1994. **265**(5168): p. 103-6.
135. Lakso, M., et al., *Targeted oncogene activation by site-specific recombination in transgenic mice.* Proc Natl Acad Sci U S A, 1992. **89**(14): p. 6232-6.
136. Denault, J.B. and G.S. Salvesen, *Human caspase-7 activity and regulation by its N-terminal peptide.* J Biol Chem, 2003. **278**(36): p. 34042-50.